

Normal variance mixtures: Distribution, density and parameter estimation

Erik Hintz¹, Marius Hofert², Christiane Lemieux³

2022-09-28

Abstract

Efficient computation of the distribution and log-density function of multivariate normal variance mixtures as well as a likelihood-based fitting procedure for those distributions are presented. Existing methods for the evaluation of the distribution function of a multivariate normal and t distribution are generalized to an efficient randomized quasi-Monte Carlo (RQMC) algorithm that is able to estimate the probability that a random vector following a multivariate normal variance mixture distribution falls into a (possibly unbounded) hyper rectangle, as long as the mixing variable has a tractable quantile function. The log-density is approximated using an adaptive RQMC algorithm. Parameter estimation for multivariate normal variance mixtures is achieved through an expectation-maximization-like algorithm where all weights and log-densities are numerically estimated. It is demonstrated through numerical examples that the suggested algorithms are quite fast; even for high dimensions around 1000 the distribution function can be estimated with moderate accuracy using only a few seconds of run time. Even log-densities around -100 can be estimated accurately and quickly. An implementation of all algorithms presented in this work is available in the R package `nmix` (version $\geq 0.0.2$).

Keywords

Multivariate normal variance mixtures, distribution functions, densities, Student t , Gauss, quasi-random number sequences.

MSC2010

62H99, 65C60

¹Department of Statistics and Actuarial Science, University of Waterloo, 200 University Avenue West, Waterloo, ON, N2L 3G1, erik.hintz@uwaterloo.ca.

²Department of Statistics and Actuarial Science, University of Waterloo, 200 University Avenue West, Waterloo, ON, N2L 3G1, marius.hofert@uwaterloo.ca. The author would like to thank NSERC for financial support for this work through Discovery Grant RGPIN-5010-2015.

³Department of Statistics and Actuarial Science, University of Waterloo, 200 University Avenue West, Waterloo, ON, N2L 3G1, cllemieux@uwaterloo.ca. The author would like to thank NSERC for financial support for this work through Discovery Grant RGPIN-238959.

1 Introduction

Normal variance mixtures such as the multivariate normal and (Student) t distributions belong to the most widely used multivariate distributions in applications in statistics, finance, insurance and risk management. Due to randomization (mixing) of the covariance matrix of a multivariate normal distribution, normal variance mixtures can achieve a much larger range of distributions than the multivariate normal, with different (joint and marginal) tail behavior including tail dependence. This makes normal variance mixtures better suited, for example, for log-return distributions, while keeping many of the advantages of multivariate normal distributions such as closedness with respect to linear combinations; see McNeil et al. (2015, Section 6.2) for more details.

A random vector $\mathbf{X} = (X_1, \dots, X_d)$ follows a *normal variance mixture*, denoted $\mathbf{X} \sim \text{NVM}_d(\boldsymbol{\mu}, \Sigma, F_W)$, if, in distribution,

$$\mathbf{X} = \boldsymbol{\mu} + \sqrt{W} \mathbf{A} \mathbf{Z}, \quad (1)$$

where $\boldsymbol{\mu} \in \mathbb{R}^d$ denotes the *location (vector)*, $\Sigma = \mathbf{A} \mathbf{A}^\top$ for $\mathbf{A} \in \mathbb{R}^{d \times k}$ is the *scale (matrix)* (a covariance matrix), and $W \sim F_W$ is a non-negative random variable independent of $\mathbf{Z} \sim \text{N}_k(\mathbf{0}, I_k)$ (where $I_k \in \mathbb{R}^{k \times k}$ denotes the identity matrix); see, for example, McNeil et al. (2015, Section 6.2). Note that $(\mathbf{X} | W) \sim \text{N}_d(\boldsymbol{\mu}, W\Sigma)$, hence the name of this class of distributions. This implies that if $\mathbb{E}(\sqrt{W}) < \infty$, then $\mathbb{E}(\mathbf{X}) = \boldsymbol{\mu}$, and if $\mathbb{E}(W) < \infty$, then $\text{cov}(\mathbf{X}) = \mathbb{E}(W)\Sigma$ and $\text{corr}(\mathbf{X}) = P$ (the correlation matrix corresponding to Σ). Furthermore, note that in the latter case with $\mathbf{A} = I_d$ (so when the components of \mathbf{X} are uncorrelated) the components of \mathbf{X} are independent if and only if W is constant almost surely and thus \mathbf{X} multivariate normal; see McNeil et al. (2015, Lemma 6.5). In what follows we focus on the case $k = d$ in which \mathbf{A} is typically the Cholesky factor computed from a given Σ ; other decompositions of Σ into $\mathbf{A} \mathbf{A}^\top$ for some $\mathbf{A} \in \mathbb{R}^{d \times d}$ can be obtained from the eigendecomposition or singular-value decomposition.

Working with normal variance mixtures (as with any other multivariate distribution) often involves four tasks: sampling, computing the joint distribution function, computing the joint density function as well as parameter estimation. Sampling is straightforward via (1) based on the Cholesky factor \mathbf{A} of Σ . This procedure is available via `rnvmix()` of the R package `nvmmix`. In contrast, evaluating the distribution or density function of normal variance mixtures is typically challenging. For example, the R package `mvtnorm` (one of the most widely used packages according to reverse depends, see Eddelbuettel (2012)) and other R packages do not even provide functionality for evaluating the distribution function of the well-known multivariate t distribution for non-integer degrees of freedom $\nu > 0$.

Given any quantile function $F_W^\leftarrow(\cdot)$ of some random variable $W \geq 0$, our work addresses the following questions:

- 1) How can we estimate the distribution function of \mathbf{X} in (1)?
- 2) How can the (log-)density function of \mathbf{X} in (1) be estimated efficiently?

- 3) How can the parameters $\boldsymbol{\mu}$, Σ and the mixing-parameters of W be estimated given an independent and identically distributed (iid) sample $\mathbf{X}_1, \dots, \mathbf{X}_n$ from $\text{NVM}_d(\boldsymbol{\mu}, \Sigma, F_W)$ using the likelihood function?

Evaluating multivariate distribution functions (such as the normal and the t) is a difficult, yet important problem that has gained much attention in the last couple of decades; see, for instance, Genz (1992), Hickernell and Hong (1997), Genz and Bretz (1999), Genz and Bretz (2002), Genz and Bretz (2009) as well as references therein for a discussion of the estimation of multivariate normal and t probabilities and recent work in Botev and L'Écuyer (2015) for the evaluation of truncated multivariate t distributions. To answer the first question given above, we generalize methods by A. Genz and F. Bretz to evaluate the distribution function of the multivariate normal and t distribution to obtain a RQMC algorithm suited for any normal variance mixture (including the case when Σ is singular) whose mixing variable admits a tractable quantile function. We also generalize a variable reordering algorithm originally suggested by Gibson et al. (1994) and adapted by Genz and Bretz (2002) which significantly reduces the variance of the integrand yielding fast convergence of our estimators.

We tackle the second question by employing an adaptive RQMC algorithm that samples mostly in certain important subdomains of the range of the mixing variable to efficiently estimate the log-density of a multivariate normal variance mixture. Even log-densities around -100 can be estimated efficiently.

For a likelihood-based fitting procedure to address the third question, we employ an ECME (“Expectation/Conditional Maximization Either”) algorithm as developed in Liu and Rubin (1994), where all weights and log-densities are estimated using RQMC methods.

All presented algorithms are available in our R package `nvmmix` (in particular, via `rnvmix()`, `pnmvmix()`, `dnvmix()` and `fitnvmix()`) and the conducted simulations are reproducible with the demo `numerical_experiments`.

To the best of our knowledge, none of the three aforementioned problems have been discussed in the literature in such generality where only the quantile function of the mixing variable W is available. By specifying the latter, methods developed in this paper (and the implementation in `nvmmix`) can be used to perform standard modeling tasks for multivariate normal variance mixtures well beyond the case of a multivariate t distribution. An example of this is given at the end of Section 7 where a multivariate financial data set is also analyzed for a Pareto-mixture.

The paper is organized as follows. Section 2 provides more details on normal variance mixtures and material required for the subsequent sections. Section 3 addresses the computation of the distribution function of normal variance mixtures and Section 4 the computation of the log-density function. In Section 5 we discuss how $\boldsymbol{\mu}$, Σ and the parameters of W can be estimated given an iid sample $\mathbf{X}_1, \dots, \mathbf{X}_n$ from $\text{NVM}_d(\boldsymbol{\mu}, \Sigma, F_W)$. In Section 6 we briefly discuss gamma-scale mixture models which are distributions derived from the Mahalanobis distance of \mathbf{X} in (1). Section 7 details an extensive numerical study for all algorithms presented as well as a data analysis with real-world financial data.

Section 8 provides concluding remarks.

2 Normal variance mixture distribution function and density

We assume that Σ has full rank so that the density of $\mathbf{X} \sim \text{NVM}_d(\boldsymbol{\mu}, \Sigma, F_W)$ exists. Denote by $D^2(\mathbf{x}; \boldsymbol{\mu}, \Sigma) = (\mathbf{x} - \boldsymbol{\mu})^\top \Sigma^{-1}(\mathbf{x} - \boldsymbol{\mu})$ the (squared) Mahalanobis distance of $\mathbf{x} \in \mathbb{R}^d$ from $\boldsymbol{\mu}$ with respect to (wrt) Σ . By conditioning on W and substituting $w = F_W^\leftarrow(u)$ (where $F_W^\leftarrow(u) = \inf\{w \in [0, \infty) : F_W(w) \geq u\}$, $u \in (0, 1)$, denotes the quantile function of F_W), the density of \mathbf{X} can then be written as

$$\begin{aligned} f_{\mathbf{X}}(\mathbf{x}) &= \int_0^\infty f_{\mathbf{X}|W}(\mathbf{x} | w) \, dF_W(w) \\ &= \int_0^\infty \frac{1}{\sqrt{(2\pi w)^d |\Sigma|}} \exp\left(-\frac{D^2(\mathbf{x}; \boldsymbol{\mu}, \Sigma)}{2w}\right) \, dF_W(w) \end{aligned} \quad (2)$$

$$= \int_0^1 \frac{1}{\sqrt{(2\pi F_W^\leftarrow(u))^d |\Sigma|}} \exp\left(-\frac{D^2(\mathbf{x}; \boldsymbol{\mu}, \Sigma)}{2F_W^\leftarrow(u)}\right) \, du. \quad (3)$$

Note that this representation holds for the case when W is absolutely continuous, discrete or of mixed type. In the former case, (2) equals

$$f_{\mathbf{X}}(\mathbf{x}) = \int_0^\infty \frac{1}{\sqrt{(2\pi w)^d |\Sigma|}} \exp\left(-\frac{D^2(\mathbf{x}; \boldsymbol{\mu}, \Sigma)}{2w}\right) f_W(w) \, dw, \quad (4)$$

where f_W denotes the density of W .

Furthermore, note that $f_{\mathbf{X}}(\mathbf{x})$ is decreasing in the Mahalanobis distance $D^2(\mathbf{x}; \boldsymbol{\mu}, \Sigma)$. Thus

$$f_{\mathbf{X}}(\mathbf{x}) \leq f_{\mathbf{X}}(\boldsymbol{\mu}) = \frac{1}{\sqrt{(2\pi)^d |\Sigma|}} \mathbb{E}\left(\frac{1}{W^{d/2}}\right); \quad \mathbf{x} \in \mathbb{R}^d$$

so that $f_{\mathbf{X}}(\mathbf{x})$ is bounded if and only if $\mathbb{E}(W^{-d/2}) < \infty$.

Let $F_{\mathbf{X}}(\mathbf{a}, \mathbf{b})$ denote the probability that \mathbf{X} falls into the hyperrectangle spanned by the lower-left endpoint \mathbf{a} and upper-right endpoint \mathbf{b} , where $\mathbf{a}, \mathbf{b} \in \bar{\mathbb{R}}^d$ for $\bar{\mathbb{R}} = \mathbb{R} \cup \{-\infty, \infty\}$ and $\mathbf{a} < \mathbf{b}$ (interpreted componentwise), where we interpret non-finite components as the corresponding limits. Note that the joint distribution function of \mathbf{X} is a special case of $F_{\mathbf{X}}(\mathbf{a}, \mathbf{b})$ since $F_{\mathbf{X}}(\mathbf{x}) := \mathbb{P}(\mathbf{X} \leq \mathbf{x}) = F_{\mathbf{X}}(\mathbf{a}, \mathbf{x})$ for $\mathbf{a} = (-\infty, \dots, -\infty)$.

In what follows we write $F(\mathbf{a}, \mathbf{b})$ instead of $F_{\mathbf{X}}(\mathbf{a}, \mathbf{b})$ to simplify notation. For computing $F(\mathbf{a}, \mathbf{b})$ assume (potentially after adjusting \mathbf{a}, \mathbf{b}) that $\boldsymbol{\mu} = \mathbf{0}$ and that Σ has full rank (the singular case will be discussed in Section 3.4). By conditioning and the substitution

3 Computing the distribution function

$w = F_W^\leftarrow(u)$ we obtain that

$$\begin{aligned} F_X(\mathbf{a}, \mathbf{b}) &= \mathbb{P}(\mathbf{a} < \mathbf{X} \leq \mathbf{b}) = \mathbb{P}(\mathbf{a} \leq \sqrt{W} \mathbf{A} \mathbf{Z} \leq \mathbf{b}) = \mathbb{E} \left(\mathbb{P}(\mathbf{a}/\sqrt{W} \leq \mathbf{A} \mathbf{Z} \leq \mathbf{b}/\sqrt{W} \mid W) \right) \\ &= \mathbb{E} \left(\Phi_\Sigma(\mathbf{a}/\sqrt{W}, \mathbf{b}/\sqrt{W}) \right) = \int_0^\infty \Phi_\Sigma(\mathbf{a}/\sqrt{w}, \mathbf{b}/\sqrt{w}) dF_W(w) \\ &= \int_0^1 \Phi_\Sigma \left(\mathbf{a}/\sqrt{F_W^\leftarrow(u)}, \mathbf{b}/\sqrt{F_W^\leftarrow(u)} \right) du, \end{aligned} \quad (5)$$

where $\Phi_\Sigma(\mathbf{a}, \mathbf{b}) = \mathbb{P}(\mathbf{a} < \mathbf{Y} \leq \mathbf{b})$ for $\mathbf{Y} \sim N_d(\mathbf{0}, \Sigma)$.

3 Computing the distribution function

Throughout the remainder of the paper assume that the quantile function F_W^\leftarrow of W is computationally tractable (possibly through an approximation).

One might be tempted to sample $U_i \stackrel{\text{ind.}}{\sim} U(0, 1)$, $i = 1, \dots, n$, and then approximate the integral in (5) by the conditional Monte Carlo estimator

$$F(\mathbf{a}, \mathbf{b}) \approx \mu_F^{\text{CMC}} = \frac{1}{n} \sum_{i=1}^n \Phi_\Sigma \left(\mathbf{a}/\sqrt{F_W^\leftarrow(U_i)}, \mathbf{b}/\sqrt{F_W^\leftarrow(U_i)} \right).$$

However, Φ_Σ itself is a d -dimensional integral typically evaluated by RQMC methods, so this approach would be time-consuming. Hence, the first step should be to approximate Φ_Σ . To this end, we follow Genz (1992) (see also Genz and Bretz (1999), Genz and Bretz (2002) and Genz and Bretz (2009)) and start by expressing Φ_Σ (and then $F(\mathbf{a}, \mathbf{b})$) as integrals over the unit hypercube. In the second part of this section, we derive an efficient randomized quasi-Monte Carlo algorithm to approximate $F(\mathbf{a}, \mathbf{b})$. The third part details how a significant variance reduction (and hence decrease in run time) can be achieved through a variable reordering following an approach originally suggested by Gibson et al. (1994) for multivariate normal probabilities and later adapted by Genz and Bretz (2002) to work for multivariate t probabilities. The last section discusses the evaluation of singular normal variance mixtures.

3.1 Reformulation of the integral

We now address Φ_Σ . Let $C = (C_{ij})_{i,j=1}^d$ be the Cholesky factor of Σ , i.e., a lower triangular matrix satisfying $CC^\top = \Sigma$. Denote by C_k^\top the k th row of C for $k = 1, \dots, d$. Genz (1992) uses a series of transformations that rely on the lower triangular structure of C to produce

3 Computing the distribution function

a separation of variables as follows:

$$\begin{aligned}
\Phi_{\Sigma}(\mathbf{a}, \mathbf{b}) &= \int_{a_1}^{b_1} \cdots \int_{a_d}^{b_d} \frac{1}{\sqrt{(2\pi)^d |\Sigma|}} \exp\left(-\frac{\mathbf{x}^\top \Sigma^{-1} \mathbf{x}}{2}\right) d\mathbf{x} \\
&= \int_{\mathbf{a} < C\mathbf{y} \leq \mathbf{b}} \phi(y_1) \cdots \phi(y_d) dy_d \cdots dy_1 \\
&= \int_{\tilde{d}_1}^{\tilde{e}_1} \cdots \int_{\tilde{d}_d}^{\tilde{e}_d} 1 dz_d \cdots dz_1 = (\hat{e}_1 - \hat{d}_1) \int_0^1 (\hat{e}_2 - \hat{d}_2) \cdots \int_0^1 (\hat{e}_d - \hat{d}_d) \int_0^1 du_d du_{d-1} \cdots du_1;
\end{aligned} \tag{6}$$

where

$$\begin{aligned}
\tilde{d}_1 &= \Phi\left(\frac{a_1}{C_{11}}\right), \quad \tilde{d}_i = \tilde{d}_i(z_1, \dots, z_{i-1}) = \Phi\left(\frac{1}{C_{ii}} \left(a_i - \sum_{j=1}^{i-1} C_{ij} \Phi^{-1}(z_j)\right)\right), \quad i = 2, \dots, d, \\
\tilde{e}_1 &= \Phi\left(\frac{b_1}{C_{11}}\right), \quad \tilde{e}_i = \tilde{e}_i(z_1, \dots, z_{i-1}) = \Phi\left(\frac{1}{C_{ii}} \left(b_i - \sum_{j=1}^{i-1} C_{ij} \Phi^{-1}(z_j)\right)\right), \quad i = 2, \dots, d;
\end{aligned} \tag{7}$$

$\hat{d}_i = \hat{d}_i(u_1, \dots, u_{i-1})$ as well as $\hat{e}_i = \hat{e}_i(u_1, \dots, u_{i-1})$ arise from \tilde{d}_i and \tilde{e}_i by a location-scale transform, i.e., by replacing z_j by $\hat{d}_j + u_j(\hat{e}_j - \hat{d}_j)$. Here, $\Phi(x) = \int_{-\infty}^x \exp(-t^2/2)/\sqrt{2\pi} dt$ denotes the distribution function of a univariate standard normal distribution $N(0, 1)$ and Φ^{-1} its quantile function. Note that the innermost integral in (6) is always $\int_0^1 du_d = 1$ so that only a $(d-1)$ dimensional integral needs to be approximated.

With this at hand, we can write (5) as

$$F(\mathbf{a}, \mathbf{b}) = \int_0^1 \int_{d_1^*}^{e_1^*} \cdots \int_{d_d^*}^{e_d^*} dz_d \cdots dz_1 du_0 \tag{8}$$

$$= \int_0^1 g_1(u_0) \int_0^1 g_2(u_0, u_1) \cdots \int_0^1 g_d(u_0, \dots, u_{d-1}) du_{d-1} \cdots du_0, \tag{9}$$

where in (8) $d_i^* = d_i^*(u_0, z_1, \dots, z_{i-1})$ and $e_i^* = e_i^*(u_0, z_1, \dots, z_{i-1})$ are \tilde{d}_i and \tilde{e}_i from (7) with a_i and b_i replaced by $a_i/\sqrt{F_W^{\leftarrow}(u_0)}$ and $b_i/\sqrt{F_W^{\leftarrow}(u_0)}$, respectively. In (9), the functions g_i are defined by

$$g_i(u_0, \dots, u_{i-1}) = e_i - d_i, \quad i = 1, \dots, d, \tag{10}$$

where d_i are recursively defined by

$$\begin{aligned}
d_1 &= d_1(u_0) = \Phi\left(\frac{a_1}{C_{11}\sqrt{F_W^{\leftarrow}(u_0)}}\right) \\
d_i &= d_i(u_0, \dots, u_{i-1}) = \Phi\left(\frac{1}{C_{ii}} \left(\frac{1}{\sqrt{F_W^{\leftarrow}(u_0)}} a_i - \sum_{j=1}^{i-1} C_{ij} \Phi^{-1}(d_j + u_j(e_j - d_j))\right)\right)
\end{aligned} \tag{11}$$

3 Computing the distribution function

for $i = 2, \dots, d$ and the e_i are d_i with a_i replaced by b_i for $i = 1, \dots, n$. We remark that there is a typo (wrong bracket) in the corresponding formula for the special case of a multivariate t distribution in Genz and Bretz (2002, p. 958).

Summarizing, the original $(d + 1)$ dimensional integral is reduced to

$$F(\mathbf{a}, \mathbf{b}) = \int_{(0,1)^d} g(\mathbf{u}) d\mathbf{u},$$

where

$$g(\mathbf{u}) = \prod_{j=1}^d g_j(u_0, \dots, u_{j-1}), \quad \mathbf{u} = (u_0, \dots, u_{d-1}) \in (0, 1)^d, \quad (12)$$

with g_1, \dots, g_d as in (10). A probabilistic interpretation of the quantities involved will be given in Remark 3.3.

3.2 Monte Carlo and quasi-Monte Carlo methods

As demonstrated in the previous section, we need to approximate $F(\mathbf{a}, \mathbf{b}) = \int_{(0,1)^d} g(\mathbf{u}) d\mathbf{u}$. If $\mathbf{U} \sim \text{U}(0, 1)^d$, we obtain that $\mu := \mathbb{E}(g(\mathbf{U})) = F(\mathbf{a}, \mathbf{b})$ which motivates the crude Monte Carlo estimator

$$F(\mathbf{a}, \mathbf{b}) \approx \hat{\mu}_F^{\text{MC, Cr}} = \frac{1}{n} \sum_{i=1}^n g(\mathbf{U}_i),$$

for μ where $\mathbf{U}_i \stackrel{\text{ind.}}{\sim} \text{U}(0, 1)^d$, $i = 1, \dots, d$. A commonly used variance reduction technique is to employ *antithetic variates* (AV): Replacing $g(\mathbf{U}_i)$ by the average of $g(\mathbf{U}_i)$ and $g(\mathbf{1} - \mathbf{U}_i)$ where $\mathbf{1} = (1, \dots, 1)$ yields the estimator

$$F(\mathbf{a}, \mathbf{b}) \approx \hat{\mu}_F^{\text{MC, AV}} = \frac{1}{n} \sum_{i=1}^n (g(\mathbf{U}_i) + g(\mathbf{1} - \mathbf{U}_i))/2. \quad (13)$$

To get a measurement of how accurate this approximation is, one can estimate the standard deviation of the Monte Carlo estimator via

$$\hat{\sigma}_{\mu_F^{\text{MC, AV}}} = \sqrt{\frac{1}{n(n-1)} \sum_{i=1}^n \left((g(\mathbf{U}_i) + g(\mathbf{1} - \mathbf{U}_i))/2 - \hat{\mu}_F^{\text{MC, AV}} \right)^2}.$$

From the central limit theorem, an approximate $(1 - p) \times 100\%$ confidence interval for the true but unknown μ is then given by

$$[\hat{\mu}_F^{\text{MC, AV}} - z_{p/2} \hat{\sigma}_{\mu_F^{\text{MC, AV}}}, \hat{\mu}_F^{\text{MC, AV}} + z_{p/2} \hat{\sigma}_{\mu_F^{\text{MC, AV}}}], \quad (14)$$

3 Computing the distribution function

where $z_{p/2} = \Phi^{-1}(1 - p/2)$. Now one can use the estimator in (13) and increase n until the length of the confidence interval (14) (or, equivalently, $\hat{\sigma}_{\mu_F^{\text{MC,AV}}}$) has reached some desired tolerance; for example, $3.5 \hat{\sigma}_{\mu_F^{\text{MC,AV}}} < \varepsilon$ with $\varepsilon = 10^{-3}$ which guarantees that the 99.95% confidence interval in (14) has halfwidth smaller than ε so that the absolute error is smaller than ε .

As noted in Genz and Bretz (2002), a great improvement in efficiency can be achieved when (pseudo-)random numbers are replaced by quasi-random numbers to generate the \mathbf{U}_i 's. Pseudo-random point sets inevitably have some parts of the domain that are oversampled and other parts which are undersampled. To overcome this issue, *quasi-Monte Carlo (QMC)* methods move away from using random input point sets and employ deterministic point sets, called low-discrepancy point sets, which fill the unit hypercube in a more homogeneous way. Let $P_n = \{\mathbf{v}_1, \dots, \mathbf{v}_n\}$ be such a point set. While QMC methods do not allow for a simple error estimation due to their deterministic nature of P_n , *randomized quasi-Monte Carlo (RQMC)* start from a (deterministic) low-discrepancy point set P_n and randomize it in a way such that the resulting point set \tilde{P}_n is uniformly distributed over $[0, 1]^d$ without losing the low-discrepancy of the point set overall. One way to do so is to set $\tilde{P}_n = \{\mathbf{u}_1, \dots, \mathbf{u}_n\}$ where $\mathbf{u}_i = (\mathbf{v}_i + \mathbf{U}) \bmod 1$, $i = 1, \dots, n$ and $\mathbf{U} \sim \text{U}(0, 1)^d$; i.e., the whole point set P_n is shifted by the same random vector \mathbf{U} . This method is usually referred to as *random shift* and was introduced in Cranley and Patterson (1976).

Throughout this work, we use a Sobol' sequence (Sobol' (1967)) as implemented in the R package `qrng` of Hofert and Lemieux (2016); in this case, generating P_n is faster than R's default (pseudo-)random number generator, the Mersenne Twister. For digital sequences such as the Sobol' sequence, the randomization scheme used is a *digital shift*, which is essentially a random shift performed on the base 2 expansions of \mathbf{v}_i and \mathbf{U} ; this is efficient as Sobol' points are generated on the level of binary expansions anyway. For more about (R)QMC methods, see for instance Lemieux (2009, Ch. 5, 6) and Glasserman (2013, Ch. 6).

Given B independently randomized versions of P_n , say $\tilde{P}_{n,b} = \{\mathbf{u}_{1,b}, \dots, \mathbf{u}_{n,b}\}$ for $b = 1, \dots, B$, we construct B independent estimators of the form

$$\hat{\mu}_{F,b}^{\text{RQMC,AV}} = \frac{1}{n} \sum_{i=1}^n (g(\mathbf{u}_{i,b}) + g(\mathbf{1} - \mathbf{u}_{i,b}))/2, \quad b = 1, \dots, B,$$

and combine them to the RQMC estimator

$$\hat{\mu}_F^{\text{RQMC,AV}} = \frac{1}{B} \sum_{b=1}^B \hat{\mu}_{F,b}^{\text{RQMC,AV}}$$

of μ . The standard deviation of $\mu_F^{\text{RQMC,AV}}$ can then be estimated via

$$\hat{\sigma}_{\mu_F^{\text{RQMC,AV}}} = \sqrt{\frac{1}{B(B-1)} \sum_{b=1}^B \left(\hat{\mu}_{F,b}^{\text{RQMC,AV}} - \hat{\mu}_F^{\text{RQMC,AV}} \right)^2}.$$

3 Computing the distribution function

As in the crude Monte Carlo approach, one can increase n until this standard deviation is sufficiently small. Since the randomization is only done to get an estimate of the variance of $\hat{\mu}_F^{\text{RQMC,AV}}$, we use a small number of $B = 15$ randomizations in our applications. Algorithm 3.1 summarizes our implementation of the estimator $\hat{\mu}_F^{\text{RQMC,AV}}$ of $F(\mathbf{a}, \mathbf{b})$ in the function `pnmix()` of the R package `nvmix`. The user can pre-specify some absolute error tolerance $\varepsilon > 0$. The algorithm then runs until $3.5 \hat{\sigma}_{\mu_F^{\text{RQMC,AV}}} < \varepsilon$.

We recycle function evaluations from iterations that did not meet the tolerance as follows. Let $P_{n_1, n_2} = \{\mathbf{v}_{n_1+1}, \dots, \mathbf{v}_{n_1+n_2}\}$ be the point set consisting of the n_2 low-discrepancy points after skipping the first n_1 -many points. Furthermore, let $\tilde{P}_{n_1, n_2, b} = \{\mathbf{u}_{n_1+1, b}, \dots, \mathbf{u}_{n_1+n_2, b}\}$ be the b th randomly shifted version of P_{n_1, n_2} and let

$$\hat{\mu}_{F, b, n_1, n_2}^{\text{RQMC,AV}} = \frac{1}{n_2} \sum_{\mathbf{u} \in \tilde{P}_{n_1, n_2, b}} (g(\mathbf{u}) + g(\mathbf{1} - \mathbf{u}))/2.$$

If n_1 points were not sufficient to meet the tolerance, an estimator based on $n_1 + n_2$ points can be calculated using only n_2 additional function evaluations via

$$\hat{\mu}_{F, b, 0, n_2}^{\text{RQMC,AV}} = \frac{n_1 \times \hat{\mu}_{F, b, 0, n_1}^{\text{RQMC,AV}} + n_2 \times \hat{\mu}_{F, b, n_1, n_2}^{\text{RQMC,AV}}}{n_1 + n_2}.$$

This is being done in Step 4.2) of Algorithm 3.1 with $n_1 = n_2 = n$.

Algorithm 3.1 (RQMC Algorithm to estimate $F(\mathbf{a}, \mathbf{b})$)

Given $\mathbf{a}, \mathbf{b}, \Sigma, \varepsilon, B$, estimate $F(\mathbf{a}, \mathbf{b})$ via:

- 1) Set n sufficiently large (eg $n = 128$).
- 2) Let $\hat{\mu}_{F, b}^{\text{RQMC,AV}} = \hat{\mu}_{F, b, 0, n}^{\text{RQMC,AV}}, b = 1, \dots, B$ and $\hat{\mu}_F^{\text{RQMC,AV}} = \frac{1}{B} \sum_{b=1}^B \hat{\mu}_{F, b}^{\text{RQMC,AV}}$.
- 3) Set $\hat{\sigma}_{\mu_F^{\text{RQMC,AV}}} = \sqrt{\frac{1}{B(B-1)} \sum_{b=1}^B \left(\hat{\mu}_{F, b}^{\text{RQMC,AV}} - \hat{\mu}_F^{\text{RQMC,AV}} \right)^2}$ and $\hat{\varepsilon} = 3.5 \hat{\sigma}_{\mu_F^{\text{RQMC,AV}}}$.
- 4) While $\hat{\varepsilon} > \varepsilon$, do:
 - 4.1) Calculate $\hat{\mu}_{F, b, n, n}^{\text{RQMC,AV}}, b = 1, \dots, B$.
 - 4.2) Update $\hat{\mu}_{F, b}^{\text{RQMC,AV}} = (\hat{\mu}_{F, b}^{\text{RQMC,AV}} + \hat{\mu}_{F, b, n, n}^{\text{RQMC,AV}})/2, b = 1, \dots, B$ and $\hat{\mu}_F^{\text{RQMC,AV}} = \frac{1}{B} \sum_{b=1}^B \hat{\mu}_{F, b}^{\text{RQMC,AV}}$.
 - 4.3) Update $\hat{\sigma}_{\mu_F^{\text{RQMC,AV}}} = \sqrt{\frac{1}{B(B-1)} \sum_{b=1}^B \left(\hat{\mu}_{F, b}^{\text{RQMC,AV}} - \hat{\mu}_F^{\text{RQMC,AV}} \right)^2}$ and $\hat{\varepsilon} = 3.5 \hat{\sigma}_{\mu_F^{\text{RQMC,AV}}}$.
 - 4.4) Set $n = 2n$.
- 5) Return $\hat{\mu}_F^{\text{RQMC,AV}}$.

In practice, it may sometimes be better to set a relative error tolerance rather than an absolute tolerance. This can be accomplished by using $\hat{\mu}_F^{\text{RQMC,AV}}$ as a proxy for $F(\mathbf{a}, \mathbf{b})$; that is, if a relative precision $\varepsilon_{\text{rel}} > 0$ is desired, one can replace $\hat{\varepsilon}$ in Steps 3) and 4.3) of Algorithm 3.1 by $\hat{\varepsilon}/\hat{\mu}_F^{\text{RQMC,AV}}$.

3.3 Variable reordering

Inspecting the integrand g in (8) and (9), we see that the sampled component u_j of \mathbf{u} in the j th integral affects all integration bounds k (or equivalently, all g_k) with $k > j$. From a simulation point of view, the particular value of u_1 will affect the bounds of all the remaining $d - 2$ integrals.

Observe that permuting the order in \mathbf{a} , \mathbf{b} and Σ does not affect the value of $F(\mathbf{a}, \mathbf{b})$ as long as the same permutation is applied to \mathbf{a} , \mathbf{b} and to both the rows and columns of Σ . It therefore seems to be a fruitful approach to choose a permutation of \mathbf{a} , \mathbf{b} and Σ such that the second outer integral (that is, the one with respect to u_1) has the smallest range, the third one (that is, the one with respect to u_2) such that it has the second-smallest range and so on. This has been observed in Gibson et al. (1994) in the context of calculating multivariate normal probabilities and has been adapted by Genz and Bretz (2002) to handle multivariate t integrals. As in the latter reference, one can sort the integration limits a priori according to their expected length of integration limits. This is more complicated than just ordering \mathbf{a} , \mathbf{b} and Σ according to the lengths $b_i - a_i$ (assuming all of them are finite) as the latter does not take into account the dependence of the components in \mathbf{X} .

In the following algorithm, we generalize the Gibson, Glasbey and Elston method to work for normal variance mixture distribution functions as in (9).

Algorithm 3.2 (Variable reordering)

- 1) Start with given $\mathbf{a}, \mathbf{b}, \Sigma$ and Cholesky factor C of Σ .
- 2) Calculate or approximate $\mu_{\sqrt{W}} = \mathbb{E}(\sqrt{W})$.
- 3) a) Choose the first integration variable as

$$i = \operatorname{argmin}_{j \in \{1, \dots, d\}} \left\{ \Phi \left(\frac{b_j}{\mu_{\sqrt{W}} \sqrt{\Sigma_{jj}}} \right) - \Phi \left(\frac{a_j}{\mu_{\sqrt{W}} \sqrt{\Sigma_{jj}}} \right) \right\}.$$

Swap components 1 and i of \mathbf{a} and \mathbf{b} and interchange both rows and columns of Σ corresponding to the variables i and 1.

- b) Update $C_{11} = \sqrt{\Sigma_{11}}$ and $C_{j1} = \Sigma_{j1}/C_{11}$ for $j = 1, \dots, d$. Set

$$y_1 = \frac{\int_{\hat{a}_1}^{\hat{b}_1} s \phi(s) ds}{\Phi(\hat{b}_1) - \Phi(\hat{a}_1)}$$

as expected value for u_1 , where

$$\hat{a}_1 = \frac{a_1}{\mu_{\sqrt{W}} C_{11}} \quad \text{and} \quad \hat{b}_1 = \frac{b_1}{\mu_{\sqrt{W}} C_{11}}.$$

This is the same as $\mathbb{E}(Z \mid Z \in [\hat{a}_1, \hat{b}_1])$ for $Z \sim N(0, 1)$.

- 4) For $j = 2, \dots, d$,

3 Computing the distribution function

- a) Choose the j th integration variable as

$$i = \operatorname{argmin}_{l \in \{j, \dots, d\}} \left\{ \Phi \left(\frac{\frac{b_l}{\mu\sqrt{W}} - \sum_{k=1}^{j-1} C_{lk} y_k}{\sqrt{\Sigma_{l,l} - \sum_{k=1}^{j-1} C_{lk}^2}} \right) - \Phi \left(\frac{\frac{a_l}{\mu\sqrt{W}} - \sum_{k=1}^{j-1} C_{lk} y_k}{\sqrt{\Sigma_{l,l} - \sum_{k=1}^{j-1} C_{lk}^2}} \right) \right\}.$$

Swap components i and j of \mathbf{a} and \mathbf{b} and interchange both rows and columns of Σ corresponding to variables i and j .

- b) Update $C_{jj} = \sqrt{\Sigma_{jj} - \sum_{k=1}^{j-1} C_{jk}^2}$ and $C_{lj} = \frac{1}{C_{jj}} \left(\Sigma_{lj} - \sum_{k=1}^{j-1} C_{jk} C_{lk} \right)$ for $l = j+1, \dots, d$ and set

$$y_j = \frac{\int_{\hat{a}_j}^{\hat{b}_j} s \phi(s) ds}{\Phi(\hat{b}_j) - \Phi(\hat{a}_j)}$$

where

$$\hat{a}_j = \frac{\frac{a_j}{\mu\sqrt{W}} - \sum_{k=1}^{j-1} C_{jk} y_k}{C_{jj}} \quad \text{and} \quad \hat{b}_j = \frac{\frac{b_j}{\mu\sqrt{W}} - \sum_{k=1}^{j-1} C_{jk} y_k}{C_{jj}}.$$

Algorithm 3.2 is a greedy procedure that only reorders $\mathbf{a}, \mathbf{b}, \Sigma$ (and updates the Cholesky factor C accordingly). Changing the order in \mathbf{a}, \mathbf{b} and Σ does not introduce any bias so that one can use a rather crude approximation for $\mu\sqrt{W}$ for $\mathbb{E}(\sqrt{W})$ if the true mean is not known. This can be obtained, for instance, using a small Monte Carlo simulation. Note also that variable reordering needs to be performed only once before running Algorithm 3.1 so that the cost of reordering is low compared to the overall cost of evaluating $F(\mathbf{a}, \mathbf{b})$.

In Section 7.2 it is shown through a simulation study that this (rather cheap) variable reordering can yield a great variance reduction for the RQMC algorithm, Algorithm 3.1.

Note that parallelization of our methods, i.e., estimation of $F(\mathbf{a}_i, \mathbf{b}_i)$, $i = 1, \dots, n$, simultaneously is difficult for two reasons: Reordering needs to be performed for each input $\mathbf{a}_i, \mathbf{b}_i$ separately so that Algorithm 3.2 needs to be called n times. Furthermore, the structure of the integrand g from (12) (see also (11)) does not allow for an efficient implementation of common random numbers as all quantile evaluations $\Phi^{-1}(\cdot)$ depend on the limits \mathbf{a}, \mathbf{b} so that they cannot be recycled.

Remark 3.3 (Another interpretation of the integrand)

As pointed out in Genz and Bretz (2009), the transformations undertaken in this section to produce a separation of variables essentially describe a Rosenblatt transform; see Rosenblatt (1952). We will now give a probabilistic interpretation of the integrand g from (12).

From a simulation point of view, each input $\mathbf{u} = (u_0, \dots, u_{d-1}) \sim U(0, 1)^d$ is transformed to a product of conditional probabilities: The first component, u_0 , is used to sample from the mixing variable via inversion; $g_1(u_0)$ is then the conditional probability of the first component of the random vector \mathbf{X} falling into (a_1, b_1) given that $W = F_W^{\leftarrow}(u_0)$, that is $g_1(u_0) = \mathbb{P}(X_1 \in (a_1, b_1) \mid W = F_W^{\leftarrow}(u_0))$. Next, u_1 is transformed to $y_1 = \Phi^{-1}(d_1 + u_1(e_1 - d_1))$, which is a realization of the random variable $(X_1 \mid X_1 \in (a_1, b_1), W = F_W^{\leftarrow}(u_0))$. Then, $g_2(u_0, u_1) = \mathbb{P}(X_2 \in (a_2, b_2) \mid X_1 = y_1, W = F_W^{\leftarrow}(u_0))$ and so on and so forth.

3 Computing the distribution function

As we are conditioning on events of the form $\{X_1 = y_1, \dots, X_l = y_l, W = F_W^{\leftarrow}(u_0)\}$ for all subsequent probabilities, this also explains why variable reordering can help decrease the variance: It is designed in a way so that X_1 has smallest (expected) range, X_2 second smallest and so on. In the explanation above, if $b_1 - a_1$ is small, there is only little variability in y_1 so that $g(u_0, u_1)$ should be close to $\mathbb{P}(X_2 \in (a_2, b_2) \mid X_1 \in (a_1, b_1), W = F_W^{\leftarrow}(u_0))$.

We point out that if $F_W^{\leftarrow}(u)$ is a non-zero constant for all $u \in (0, 1)$ (corresponding to \mathbf{X} being multivariate normal), this is the original derivation in Gibson et al. (1994) who independently developed a Monte Carlo procedure to approximate multivariate normal probabilities similar to Genz (1992).

3.4 Evaluating singular normal variance mixtures

We now address the case of a singular normal variance mixture, that is, we assume that $\Sigma \in \mathbb{R}^{d \times d}$ is positive semidefinite with rank $1 \leq r < d$. We can directly apply results described in Genz and Kwong (2000), who developed an accurate method to evaluate the distribution function of a multivariate normal distribution with singular correlation matrix Σ , see also Genz and Bretz (2009, Section 5.2) for more details.

Let $\Sigma = CC^\top$ with $C_{ij} = 0$ for $j > r$, $i = 1, \dots, d$, that is, C is lower triangular with some diagonal elements being zero; see Healy (1968) for an algorithm to compute such C which uses a numerical tolerance to determine zero-entries. After permutations and scalings (that must also be applied to \mathbf{a} and \mathbf{b}), C shall have the following form where “*” denotes an entry that can be zero or non-zero:

$$C = \begin{pmatrix} 1 & 0 & 0 & \dots & \dots & \dots & \dots & 0 \\ \vdots & \vdots & \vdots & \vdots & \vdots & \vdots & \vdots & \vdots \\ 1 & 0 & \dots & \dots & \dots & \dots & \dots & 0 \\ * & 1 & 0 & \dots & \dots & \dots & \dots & 0 \\ \vdots & \vdots & \vdots & \vdots & \vdots & \vdots & \vdots & \vdots \\ * & 1 & 0 & \dots & \dots & \dots & \dots & 0 \\ \vdots & \vdots & \vdots & \vdots & \vdots & \vdots & \vdots & \vdots \\ * & * & \dots & * & 1 & 0 & \dots & 0 \\ \vdots & \vdots & \vdots & \vdots & \vdots & \vdots & \vdots & \vdots \\ * & * & \dots & * & 1 & 0 & \dots & 0 \end{pmatrix} \begin{matrix} 1 \\ \vdots \\ k_1 \\ 1 \\ \vdots \\ k_2 \\ \vdots \\ 1 \\ \vdots \\ k_r \end{matrix}$$

Note that $\sum_{j=1}^r k_j = d$. Define $m_i = \sum_{j=1}^{i-1} k_j$ with $m_1 = 0$. As demonstrated in Genz and Kwong (2000), Φ_Σ can then be written in a similar fashion as in (6):

$$\Phi_\Sigma(\mathbf{a}, \mathbf{b}) = \int_{\mathbf{a} < C\mathbf{y} \leq \mathbf{b}} \phi(y_1) \dots \phi(y_d) d\mathbf{y} = \int_{\tilde{a}_1}^{\tilde{b}_1} \phi(y_1) \dots \int_{\tilde{a}_r}^{\tilde{b}_r} \phi(y_r) dy_r \dots dy_1 \quad (15)$$

Note that the r -dimensional integral still has d active constraints: For variable l , the k_l constraints $\mathbf{a}_j < C_j^\top \mathbf{y} \leq \mathbf{b}_j$ for $j \in \{m_l + 1, \dots, m_{l+1}\}$ need to be satisfied simultaneously

4 Computing the (logarithmic) density

so that the limits in (15) are given by

$$\tilde{a}_l = \max_{m_l < i \leq m_{l+1}} \left\{ a_i - \sum_{j=1}^{l-1} C_{i,j} y_j \right\} \quad \text{and} \quad \tilde{b}_l = \min_{m_l < i \leq m_{l+1}} \left\{ b_i - \sum_{j=1}^{l-1} C_{i,j} y_j \right\}$$

for $l = 1, \dots, r$.

This idea can be generalized to singular normal variance mixtures. Proceeding as in Section 3.1 one obtains

$$F(\mathbf{a}, \mathbf{b}) = \int_{(0,1)^r} g(\mathbf{u}) \, d\mathbf{u},$$

where

$$g(\mathbf{u}) = \prod_{l=1}^r (e_l(u_0, \dots, u_{l-1}) - d_l(u_0, \dots, u_{l-1}))$$

with

$$d_l(u_0, \dots, u_{l-1}) = \Phi \left(\max_{m_l < i \leq m_{l+1}} \left\{ \frac{a_i}{\sqrt{F_W^{\leftarrow}(u_0)}} - \sum_{j=1}^{l-1} C_{i,j} \Phi^{-1}(d_j + u_j(e_j - d_j)) \right\} \right),$$

$$e_l(u_0, \dots, u_{l-1}) = \Phi \left(\min_{m_l < i \leq m_{l+1}} \left\{ \frac{b_i}{\sqrt{F_W^{\leftarrow}(u_0)}} - \sum_{j=1}^{l-1} C_{i,j} \Phi^{-1}(d_j + u_j(e_j - d_j)) \right\} \right)$$

for $l = 1, \dots, r$. The methods described in Section 3.2, in particular Algorithm 3.1, can be applied to the problem in this form. The main difference is that the dimension of the problem here is given by the rank r as opposed to the dimension $d > r$ of the normal variance mixture.

4 Computing the (logarithmic) density

Let us now turn to the task of computing the (logarithmic) density function of a normal variance mixture. From (3) it follows that computing the density requires the evaluation of the univariate integral

$$f_{\mathbf{X}}(\mathbf{x}) = \int_0^1 h(u) \, du,$$

where

$$h(u) = \frac{1}{\sqrt{(2\pi F_W^{\leftarrow}(u))^d |\Sigma|}} \exp \left(-\frac{D^2(\mathbf{x}; \boldsymbol{\mu}, \Sigma)}{2F_W^{\leftarrow}(u)} \right). \quad (16)$$

To simplify notation, we write $f(\mathbf{x})$ instead of $f_{\mathbf{X}}(\mathbf{x})$ whenever confusion is not possible.

4.1 Crude Approach

As a first approach, we suggest a RQMC method rather than a quadrature rule as it allows for reliable error estimates.

As in Section 3.2, let $\tilde{P}_{n,b} = \{u_{1,b}, \dots, u_{n,b}\}$ for $b = 1, \dots, B$ denote B independent randomized copies of a one-dimensional low-discrepancy point-set P_n . Set

$$\hat{\mu}_{f,b}^{\text{RQMC}} = \frac{1}{n} \sum_{i=1}^n \frac{1}{\sqrt{(2\pi F_W^{\leftarrow}(u_{i,b}))^d |\Sigma|}} \exp\left(-\frac{D^2(\mathbf{x}; \boldsymbol{\mu}, \Sigma)}{2F_W^{\leftarrow}(u_{i,b})}\right)$$

for $b = 1, \dots, B$ so that one obtains the RQMC estimator

$$f(\mathbf{x}) \approx \hat{\mu}_f^{\text{RQMC}} = \frac{1}{B} \sum_{b=1}^B \hat{\mu}_{f,b}^{\text{RQMC}}, \quad \mathbf{x} \in \mathbb{R}^d.$$

of $f(\mathbf{x})$.

For likelihood-based methods one should compute the logarithmic density (or *log-density*) rather than the density. From a numerical point of view, it is often not a good idea to use $\log f(\mathbf{x}) \approx \log \hat{\mu}_f^{\text{RQMC}}$ directly, but rather compute a *proper logarithm*, that is, a numerically more robust estimator for $\log f(\mathbf{x})$; this is also how other densities in R are implemented. Internally, one often computes the proper logarithm by default and only returns its exponential (so the density itself) if required. To this end, we define the function LSE (for Logarithmic Sum of Exponentials) as

$$\text{LSE}(c_1, \dots, c_n) = \log\left(\sum_{i=1}^n \exp(c_i)\right) = c_{\max} + \log\left(\sum_{i=1}^n \exp(c_i - c_{\max})\right)$$

where $c_1, \dots, c_n \in \mathbb{R}$ and $c_{\max} = \max\{c_1, \dots, c_n\}$. The right hand side of the equation is numerically more stable than the left hand side as the the sum inside the logarithm is bounded between 1 and n . Applied to our problem, with

$$\begin{aligned} c_{i,b} &= \log\left(\frac{1}{\sqrt{(2\pi F_W^{\leftarrow}(u_{i,b}))^d |\Sigma|}} \exp\left(-\frac{D^2(\mathbf{x}; \boldsymbol{\mu}, \Sigma)}{2F_W^{\leftarrow}(u_{i,b})}\right)\right) \\ &= -\frac{d}{2} \log(2\pi F_W^{\leftarrow}(u_{i,b})) - \frac{1}{2} \log |\Sigma| - \frac{D^2(\mathbf{x}; \boldsymbol{\mu}, \Sigma)}{2F_W^{\leftarrow}(u_{i,b})}, \quad i = 1, \dots, n, \end{aligned}$$

the b 'th RQMC estimator is then defined as

$$\hat{\mu}_{\log f,b}^{\text{RQMC}} = -\log(n) + \text{LSE}(c_{1,b}, \dots, c_{n,b})$$

for $b = 1, \dots, B$.

Mathematically, $\hat{\mu}_{\log f,b}^{\text{RQMC}} = \log(\hat{\mu}_{f,b}^{\text{RQMC}})$ but numerically, $\hat{\mu}_{\log f,b}^{\text{RQMC}}$ is more stable, especially for large (squared) Mahalanobis distances $D^2(\mathbf{x}; \boldsymbol{\mu}, \Sigma)$ that yield very small (negative) $c_{i,b}$.

4 Computing the (logarithmic) density

Those B estimators are then combined via

$$\hat{\mu}_{\log f}^{\text{RQMC}} = -\log(B) + \text{LSE} \left(\hat{\mu}_{\log f,1}^{\text{RQMC}}, \dots, \hat{\mu}_{\log f,B}^{\text{RQMC}} \right) \quad (17)$$

which is an asymptotically unbiased estimator for $\log f(\mathbf{x})$. We remark that one could have also used the arithmetic mean of $\hat{\mu}_{\log f,1}^{\text{RQMC}}, \dots, \hat{\mu}_{\log f,B}^{\text{RQMC}}$; numerical results suggest that (17) yields more accurate results. The standard deviation of $\hat{\mu}_{\log f}^{\text{RQMC}}$ is estimated in the usual way by

$$\hat{\sigma}_{\mu_{\log f}^{\text{RQMC}}} = \sqrt{\frac{1}{B(B-1)} \sum_{b=1}^B \left(\hat{\mu}_{\log f,b}^{\text{RQMC}} - \hat{\mu}_{\log f}^{\text{RQMC}} \right)^2}.$$

The procedure is summarized in Algorithm 4.1, where the same notation as in Algorithm 3.1 is used. Again, the user specifies an absolute error tolerance $\varepsilon > 0$ for the log-density. Following the same reasoning as in the remark after Algorithm 3.1, a relative error tolerance can be specified alternatively. For later purposes and in order to bound the run time from above in case the desired precision cannot be reached quickly enough we also include a variable i_{\max} to control the maximum number of iterations.

Algorithm 4.1 (Crude RQMC algorithm to estimate $\log f(\mathbf{x})$)

Given \mathbf{x} , Σ , ε , B , i_{\max} , estimate $\log f(\mathbf{x})$ via:

- 1) Set n sufficiently large (eg $n = 128$) and $i = 1$.
- 2) Let $\hat{\mu}_{\log f,b}^{\text{RQMC}} = \hat{\mu}_{\log f,b,0,n}^{\text{RQMC}}$, $b = 1, \dots, B$ and $\hat{\mu}_{\log f}^{\text{RQMC}} = -\log(B) + \text{LSE} \left(\left\{ \hat{\mu}_{\log f,b,0,n}^{\text{RQMC}} \right\}_{b=1}^B \right)$
- 3) Compute $\hat{\sigma}_{\mu_{\log f}^{\text{RQMC}}} = \sqrt{\frac{1}{B(B-1)} \sum_{b=1}^B \left(\hat{\mu}_{\log f,b}^{\text{RQMC}} - \hat{\mu}_{\log f}^{\text{RQMC}} \right)^2}$ and set $\hat{\varepsilon} = 3.5 \hat{\sigma}_{\mu_{\log f}^{\text{RQMC}}}$.
- 4) While $\hat{\varepsilon} > \varepsilon$ and $i < i_{\max}$, do:
 - 4.1) Calculate $\hat{\mu}_{\log f,b,n,n}^{\text{RQMC}}$, $b = 1, \dots, B$.
 - 4.2) Update $\hat{\mu}_{\log f,b}^{\text{RQMC}} = -\log(2) + \text{LSE} \left(\hat{\mu}_{\log f,b}^{\text{RQMC}}, \hat{\mu}_{\log f,b,n,n}^{\text{RQMC}} \right)$, $b = 1, \dots, B$ and $\hat{\mu}_{\log f}^{\text{RQMC}} = -\log(B) + \text{LSE} \left(\left\{ \hat{\mu}_{\log f,b}^{\text{RQMC}} \right\}_{b=1}^B \right)$.
 - 4.3) Update $\hat{\sigma}_{\mu_{\log f}^{\text{RQMC}}} = \sqrt{\frac{1}{B(B-1)} \sum_{b=1}^B \left(\hat{\mu}_{\log f,b}^{\text{RQMC}} - \hat{\mu}_{\log f}^{\text{RQMC}} \right)^2}$ and $\hat{\varepsilon} = 3.5 \hat{\sigma}_{\mu_{\log f}^{\text{RQMC}}}$.
 - 4.4) Set $n = 2n$ and $i = i + 1$.
- 5) Return $\hat{\mu}_{\log f}^{\text{RQMC}}$.

Algorithm 4.1 can be vectorized easily: Given inputs $\mathbf{x}_1, \dots, \mathbf{x}_N$ one can perform all steps in Algorithm 4.1 for all inputs at once by using *the same* realizations of W , i.e., using the same $F_W^{\leftarrow}(u_{i,b})$ for all inputs \mathbf{x}_i , $i = 1, \dots, N$. The stopping criterion in Step 4) can then be replaced by $\max\{\hat{\varepsilon}_1, \dots, \hat{\varepsilon}_N\} > \varepsilon$ so that the required accuracy is guaranteed for all inputs after termination.

4 Computing the (logarithmic) density

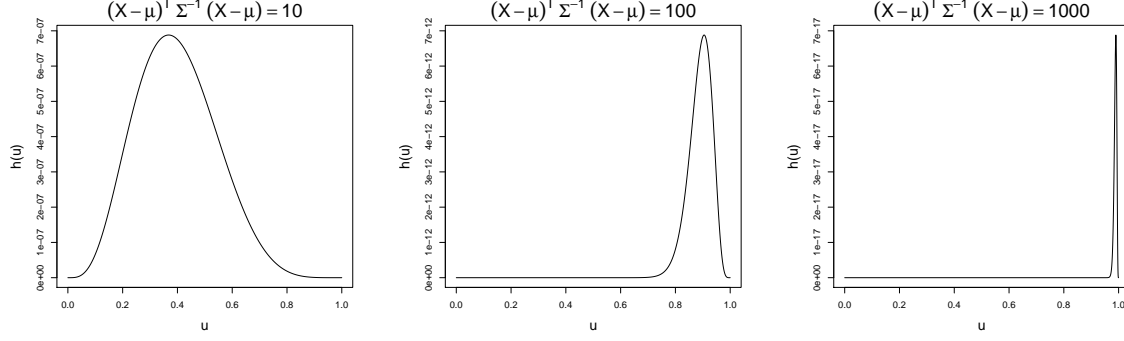


Figure 1 Integrand h for a 10-dimensional t distribution with 2 degrees of freedom.

4.2 Adaptive Procedure

Algorithm 4.1 performs sufficiently well for inputs \mathbf{x} with small to moderate Mahalanobis distances, but deteriorates for larger Mahalanobis distances. The reason is that the overall shape of the integrand, $h(u)$, is heavily influenced by $D^2(\mathbf{x}; \boldsymbol{\mu}, \Sigma)$ and for large Mahalanobis distances, most of the mass is concentrated in a small domain of $(0, 1)$. This is illustrated in Figure 1 where the integrand $h(u)$ is plotted against u in the special case of a multivariate t distribution in dimension 10 with 2 degrees of freedom. For instance, in the right-most plot, most of the mass is concentrated near 1. It thus seems to be a fruitful approach to tailor Algorithm 4.1 in a way so that it samples mostly in the relevant domain. To this end, we summarize some properties of the function h in the following lemma which can be shown using elementary calculus.

Lemma 4.2

Let W be a continuous distribution supported on the whole positive real line. Then, the function h from Equation (16) is continuous on $(0, 1)$, satisfies $h(0) = h(1) = 0$ and $h(u) > 0$ for $u \in (0, 1)$. Furthermore, the maximum value of h on $(0, 1)$, i.e., $h_{\max} = \max\{h(u) : u \in [0, 1]\}$ is attained in the interior of $(0, 1)$. The maximum is attained at

$$u^* = F_W\left(\frac{D^2(\mathbf{x}; \boldsymbol{\mu}, \Sigma)}{d}\right) \text{ with } h(u^*) = \left(\frac{2\pi|\Sigma|^{1/d} \cdot D^2(\mathbf{x}; \boldsymbol{\mu}, \Sigma)}{d}\right)^{-d/2} \exp\left(-\frac{d}{2}\right) \quad (18)$$

so that h_{\max} is independent of the distribution of W . Finally, h is strictly increasing on $(0, u^*)$ and strictly decreasing on $(u^*, 1)$.

Equation (18) is crucial for our adaptive algorithm: The value h_{\max} , i.e., the height of the peak of the integrand h , is independent of the distribution of W as long as W is continuous and supported on the whole positive real line. If W is continuous but has bounded support, h_{\max} may need to be replaced by $h(0)$ or $h(1)$. If W is discrete, the problem becomes trivial as an analytical formula for the density is available in this case.

4 Computing the (logarithmic) density

The idea is now to apply Algorithm 4.1 only to a relevant region around u^* from (18), which can be done as follows: Given a threshold ε_{th} with $0 < \varepsilon_{\text{th}} \ll h_{\text{max}}$, the structure of the integrand h guarantees the existence of u_l, u_r (l for “left” and r for “right”) with $0 < u_l < u^* < u_r < 1$ so that $h(u) > \varepsilon_{\text{th}}$ if and only if $u \in (u_l, u_r)$. For instance, take

$$\varepsilon_{\text{th}} = 10^{\log(h_{\text{max}})/\log(10) - k_{\text{th}}} \quad (19)$$

with $k_{\text{th}} = 10$ so that ε_{th} is 10 orders smaller than h_{max} . Algorithm 4.1 can then be used in the region (u_l, u_r) by replacing every number $v \in (0, 1)$ by $v' = u_l + (u_r - u_l)v \in (u_l, u_r)$. This will give an estimate for $\log \int_{u_l}^{u_r} h(u) du$. For the remaining regions $(0, u_l)$ and $(u_r, 1)$ we suggest using a crude trapezoidal rule: If $\varepsilon_{\text{th}} \ll h_{\text{max}}$ those regions do not significantly contribute to the overall integral anyway, so a rather cheap and quick procedure is recommended here.

It remains to discuss how to find u_l, u^*, u_r . Recall that the only information available about W is its quantile function F_W^{\leftarrow} in form of a “black box” so that u^* from (18) cannot be computed directly. We suggest using a bisection algorithm to solve the equivalent equation $F_W^{\leftarrow}(u) = \mathbf{x}^\top \Sigma^{-1} \mathbf{x} / d$. Starting values can be found using a small number of pilot runs. Similarly, there is no direct formula for u_l and u_r . While those can be expressed using Lambert’s W function, the lack of information about W does not allow a direct calculation. A bisection can be used here as well.

Clearly, all pilot runs and all quantile evaluations performed in the bisections should be stored so that those expensive evaluations can be re-used.

In practice, often the log-density for several inputs, say $\mathbf{x}_1, \dots, \mathbf{x}_N$ needs to be computed. This is certainly true for likelihood-based methods, where the log-density of a sample $\{\mathbf{x}_1, \dots, \mathbf{x}_N\}$ needs to be optimized over some parameter space. As this task needs to be performed quickly, any algorithm estimating the log-density should be vectorized. Vectorization was easy for Algorithm 4.1, but this is not true for the above explained procedure. Keeping Figure 1 in mind, the shape of the integrand heavily depends on \mathbf{x} through its Mahalanobis distance, and this holds true for u_l, u^*, u_r as well. In order to reduce run time, we suggest running Algorithm 4.1 on all inputs $\mathbf{x}_1, \dots, \mathbf{x}_N$ with a small number of iterations (say, $i_{\text{max}} = 4$) first and use the above procedure only for those inputs \mathbf{x}_k whose error estimates did not reach the tolerance. The advantage is that only little run time is spent on estimating “easy” integrals. Furthermore, realizations of W obtained in Algorithm 4.1 can be stored: if $i_{\text{max}} = 4$, $B = 15$ and the initial sample size is $n_0 = 128$ as in Algorithm 4.1, such pilot run gives 15 360 pairs $(u, F_W^{\leftarrow}(u))$. These can be reused to get starting values for the bisections to find u_l, u_r and u^* and they can also be used to estimate the integral in the regions $(0, u_l)$ and $(u_r, 1)$ using a trapezoidal rule with non-equidistant knots. The following algorithm summarizes our procedure.

Algorithm 4.3 (Adaptive RQMC Algorithm to estimate $\log f(\mathbf{x}_1), \dots, \log f(\mathbf{x}_N)$)

Given $\mathbf{x}_1, \dots, \mathbf{x}_N$, Σ , ε , $\varepsilon_{\text{bisec}}$, B , i_{max} , k_{th} , estimate $\log f(\mathbf{x}_l)$, $l = 1, \dots, N$, via:

- 1) Run Algorithm 4.1 with at most i_{max} iterations on all inputs \mathbf{x}_l , $l = 1, \dots, N$. Store all uniforms and corresponding quantiles $F_W^{\leftarrow}(\cdot)$ in a list, say \mathcal{L} .

4 Computing the (logarithmic) density

- 2) If all estimates $\mu_{\log f(\mathbf{x}_l)}^{\text{RQMC}}$, $l = 1, \dots, N$ meet the error tolerance ε , go to Step 4).
If not, we can assume wlog (after reordering) that \mathbf{x}_s , $s = 1, \dots, N'$ with $1 \leq N' \leq N$ are the inputs whose error estimates did not meet the error tolerance.
- 3) For each remaining input \mathbf{x}_s , $s = 1, \dots, N'$, do the following:
 - 3.1) Determine h_{\max} using (18) and ε_{th} using (19).
 - 3.2) Find maximal $u^{*,l}$ and minimal $u^{*,r}$ in the list \mathcal{L} so that $F_W^{\leftarrow}(u^{*,l}) \leq \mathbf{x}_s^\top \Sigma^{-1} \mathbf{x}_s / d \leq F_W^{\leftarrow}(u^{*,r})$ (which implies $u^{*,l} \leq u^* \leq u^{*,r}$). Use a bisection algorithm with starting values $u^{*,l}$ and $u^{*,r}$ and a tolerance of $\varepsilon_{\text{bisec}}$ to find u^* . Add any additional u 's and $F_W^{\leftarrow}(u)$'s computed in the bisection to the list \mathcal{L} .
 - 3.3) Find the largest number $u_l^{(1)} \in \mathcal{L}$ and the smallest number $u_l^{(2)} \in \mathcal{L}$ such that $u_l^{(1)} \leq u_l^{(2)} \leq u^*$, $h(u_l^{(1)}) \leq \varepsilon_{\text{th}}$ and $h(u_l^{(2)}) \geq \varepsilon_{\text{th}}$. Then $u_l^{(1)} \leq u_l \leq u_l^{(2)} \leq u^*$.
Similarly, find the largest number $u_r^{(1)} \in \mathcal{L}$ and the smallest number $u_r^{(2)} \in \mathcal{L}$ such that $u^* \leq u_r^{(1)} \leq u_r^{(2)}$, $h(u_r^{(1)}) \geq \varepsilon_{\text{th}}$ and $h(u_r^{(2)}) \leq \varepsilon_{\text{th}}$. Then $u^* \leq u_r^{(1)} \leq u_r \leq u_r^{(2)}$.
Then use a bisection to find u_l (using starting values $u_l^{(1)}$ and $u_l^{(2)}$) and u_r (using starting values $u_r^{(1)}$ and $u_r^{(2)}$) with a tolerance of $\varepsilon_{\text{bisec}}$. Add any additional u 's and $F_W^{\leftarrow}(u)$'s computed in the bisection to the list \mathcal{L} .
 - 3.4) Approximate $\log \int_0^{u_l} h(u) du$ using a trapezoidal rule with knots u'_1, \dots, u'_m where u'_i are those u 's in \mathcal{L} satisfying $u \leq u_l$. Call the approximation $\hat{\mu}_{(0,u_l)}(\mathbf{x}_s)$.
 - 3.5) Approximate $\log \int_{u_r}^1 h(u) du$ using a trapezoidal rule with knots u''_1, \dots, u''_p where u''_i are those u 's in \mathcal{L} satisfying $u \geq u_r$. Call the approximation $\hat{\mu}_{(u_r,1)}(\mathbf{x}_s)$.
 - 3.6) Run Algorithm 4.1 on \mathbf{x}_l where all uniforms $v \in (0,1)$ are replaced by $v' = u_l + (u_r - u_l)v \in (u_l, u_r)$. Call the output $\hat{\mu}$. Then set $\hat{\mu}_{(u_l,u_r)} = \log(u_r - u_l) + \hat{\mu}$ which estimates $\log \int_{u_l}^{u_r} h(u) du$.
 - 3.7) Combine
$$\mu_{\log f(\mathbf{x}_s)}^{\text{RQMC}} = \text{LSE} \left(\hat{\mu}_{(0,u_l)}(\mathbf{x}_s), \hat{\mu}_{(u_l,u_r)}(\mathbf{x}_s), \hat{\mu}_{(u_r,1)}(\mathbf{x}_s) \right)$$
- 4) Return $\mu_{\log f(\mathbf{x}_l)}^{\text{RQMC}}$, $l = 1, \dots, N$

This is what `dnvmix(, log = TRUE)` of the R package `nvmmix` computes. Using the same argument as outlined right after Algorithm 3.1, this algorithm can be easily adapted to work for relative (as opposed to absolute) error tolerances.

Remark 4.4

Algorithm 3.1 is actually able to estimate a slightly larger class of integrals. Let

$$\mu = \int_0^\infty c w^{-k} \exp(m/w) dF_W(w) = \int_0^\infty \tilde{h}(u) du;$$

here, $k, m > 0$ are constant and $\tilde{h}(u) = c F_W^{\leftarrow}(u)^{-k} \exp(m/F_W^{\leftarrow}(u))$ for $u \in (0,1)$. A result similar to Lemma 4.2 applies to \tilde{h} (replace d by k in the formula for u^* in (18)). Thus,

after only slight adjustments to Algorithm 3.1, the latter can be used to estimate $\log(\mu)$ efficiently. This will be useful in Section 5.

5 Fitting multivariate normal variance mixtures

In this section, we derive an expectation-maximization (EM) like algorithm to answer the third question in the introduction on page 2.

Assume $\mathbf{X}_1, \dots, \mathbf{X}_n \stackrel{\text{iid.}}{\sim} \text{NVM}_d(\boldsymbol{\mu}, \Sigma, F_W)$ where F_W has quantile function $F_W^{\leftarrow}(u; \boldsymbol{\nu})$ with unknown parameter vector $\boldsymbol{\nu}$ of length p_ν , unknown location vector $\boldsymbol{\mu}$ and unknown scale matrix Σ . For notational convenience, let $\boldsymbol{\theta} = (\boldsymbol{\nu}, \boldsymbol{\mu}, \Sigma^{-1})$ and denote by $\boldsymbol{\theta}_k$ the current value of $\boldsymbol{\theta}$ in iteration k .

Before deriving our algorithm, we need some notation. The original log-likelihood is given by

$$\log L^{\text{org}}(\boldsymbol{\nu}, \boldsymbol{\mu}, \Sigma; \mathbf{X}_1, \dots, \mathbf{X}_n) = \sum_{i=1}^n \log f_{\mathbf{X}}(\mathbf{X}_i; \boldsymbol{\nu}, \boldsymbol{\mu}, \Sigma)$$

and the complete log-likelihood $\log L^c$ can be written as

$$\begin{aligned} \log L^c(\boldsymbol{\theta}; \mathbf{X}_1, \dots, \mathbf{X}_n, W_1, \dots, W_n) &= \sum_{i=1}^n \log f_{\mathbf{X}, W}(\mathbf{X}_i, W_i; \boldsymbol{\theta}) \\ &= \sum_{i=1}^n \log f_{\mathbf{X}|W}(\mathbf{X}_i | W_i; \boldsymbol{\mu}, \Sigma) + \sum_{i=1}^n \log f_W(W_i; \boldsymbol{\nu}), \end{aligned} \quad (20)$$

where W_1, \dots, W_n are (unobserved) iid copies of W . Note that the first sum contains the log-likelihood contributions of $\text{N}_d(\boldsymbol{\mu}, W_i \Sigma)$ and thus is almost the log-likelihood of a normal distribution apart from potentially different W_i (expected, for example, if W is continuously distributed on the whole positive real line). The expected value of the complete log-likelihood given the (observed) data $\mathbf{X}_1, \dots, \mathbf{X}_n$ and current estimate $\boldsymbol{\theta}_k$ is then

$$Q(\boldsymbol{\theta}; \boldsymbol{\theta}_k) = \mathbb{E}(\log L^c(\boldsymbol{\theta}; \mathbf{X}_1, \dots, \mathbf{X}_n, W_1, \dots, W_n) | \mathbf{X}_1, \dots, \mathbf{X}_n; \boldsymbol{\theta}_k). \quad (21)$$

A classical EM algorithm would calculate $Q(\boldsymbol{\theta}; \boldsymbol{\theta}_k)$ from (21) in each iteration and then maximize this quantity over $\boldsymbol{\nu}$. Due to lack of knowledge of $f_W(\cdot)$ this cannot be accomplished so that instead we employ an ECME algorithm as developed in Liu and Rubin (1994); see also references therein for more details on variations of the EM algorithm. The basic structure of our algorithm is as follows:

Algorithm 5.1 (ECME Algorithm for fitting normal variance mixtures: Main idea)

Given iid data $\mathbf{X}_1, \dots, \mathbf{X}_n$, estimate $\boldsymbol{\mu}, \Sigma, \boldsymbol{\nu}$ via:

- 1) Obtain an initial estimate $\boldsymbol{\theta}_0 = (\boldsymbol{\nu}_0, \boldsymbol{\mu}_0, \Sigma_0^{-1})$

5 Fitting multivariate normal variance mixtures

2) For $k = 1, \dots$, repeat until convergence

2.1) Update $\boldsymbol{\mu}_k$ and Σ_k by maximizing $Q(\boldsymbol{\theta}; \boldsymbol{\theta}_k)$ with respect to $\boldsymbol{\mu}$ and Σ with $\boldsymbol{\nu} = \boldsymbol{\nu}_{k-1}$ held fixed.

2.2) Update $\boldsymbol{\nu}_k$ by maximizing $\log L^{\text{org}}(\boldsymbol{\nu}, \boldsymbol{\mu}_k, \Sigma_k; \mathbf{X}_1, \dots, \mathbf{X}_n)$ with respect to $\boldsymbol{\nu}$.

That is, in the k 'th iteration, we first update $\boldsymbol{\mu}$ and Σ by maximizing the expected complete log-likelihood conditional on the observed data and then update $\boldsymbol{\nu}$ by maximizing the original likelihood with respect to $\boldsymbol{\nu}$ with $\boldsymbol{\mu}$ and Σ set to their current estimates. This is an ECME algorithm as we either maximize the expected complete log-likelihood or the original likelihood; see also Liu and Rubin (1995) for a discussion of an ECME algorithm for the multivariate t distribution.

Let

$$\xi_{ki} = \mathbb{E}(\log W_i | \mathbf{X}_i; \boldsymbol{\theta}_k) \quad \text{and} \quad \delta_{ki} = \mathbb{E}(1/W_i | \mathbf{X}_i; \boldsymbol{\theta}_k), \quad i = 1, \dots, n.$$

We calculate $Q(\boldsymbol{\theta}; \boldsymbol{\theta}_k)$ from (21) in the following lemma:

Lemma 5.2

$Q(\boldsymbol{\theta}; \boldsymbol{\theta}_k)$ from (21) allows for the decomposition $Q(\boldsymbol{\theta}; \boldsymbol{\theta}_k) = Q_{\mathbf{X}|W}(\boldsymbol{\mu}, \Sigma^{-1}; \boldsymbol{\theta}_k) + Q_W(\boldsymbol{\nu}; \boldsymbol{\theta}_k)$ where

$$Q_{\mathbf{X}|W}(\boldsymbol{\mu}, \Sigma^{-1}; \boldsymbol{\theta}_k) = -\frac{1}{2} \left(nd \log(2\pi) - n \log(\det(\Sigma^{-1})) + \sum_{i=1}^n (D^2(\mathbf{X}_i; \boldsymbol{\mu}, \Sigma) \delta_{ki} + d \xi_{ki}) \right),$$

$$Q_W(\boldsymbol{\nu}; \boldsymbol{\theta}_k) = \sum_{i=1}^n \mathbb{E}(\log f_W(W_i; \boldsymbol{\nu}) | \mathbf{X}_i; \boldsymbol{\theta}_k).$$

Proof. Starting from (21) and using (20) we obtain

$$\begin{aligned} & Q(\boldsymbol{\theta}; \boldsymbol{\theta}_k) \\ &= \mathbb{E}(\log L^c(\boldsymbol{\theta}; \mathbf{X}_1, \dots, \mathbf{X}_n, W_1, \dots, W_n) | \mathbf{X}_1, \dots, \mathbf{X}_n; \boldsymbol{\theta}_k) \\ &= \sum_{i=1}^n \mathbb{E}(\log f_{\mathbf{X}|W}(\mathbf{X}_i | W_i; \boldsymbol{\mu}, \Sigma) | \mathbf{X}_1, \dots, \mathbf{X}_n; \boldsymbol{\theta}_k) + \sum_{i=1}^n \mathbb{E}(\log f_W(W_i; \boldsymbol{\nu}) | \mathbf{X}_1, \dots, \mathbf{X}_n; \boldsymbol{\theta}_k) \\ &= \sum_{i=1}^n \mathbb{E}(\log f_{\mathbf{X}|W}(\mathbf{X}_i | W_i; \boldsymbol{\mu}, \Sigma) | \mathbf{X}_i; \boldsymbol{\theta}_k) + \sum_{i=1}^n \mathbb{E}(\log f_W(W_i; \boldsymbol{\nu}) | \mathbf{X}_i; \boldsymbol{\theta}_k) \\ &= Q_{\mathbf{X}|W}(\boldsymbol{\mu}, \Sigma^{-1}; \boldsymbol{\theta}_k) + Q_W(\boldsymbol{\nu}; \boldsymbol{\theta}_k) \end{aligned}$$

where the first expectation is taken with respect to W_1, \dots, W_n for given $\mathbf{X}_1, \dots, \mathbf{X}_n$ and $\boldsymbol{\theta}_k$, and the last line of the displayed equation is understood as the definition of $Q_{\mathbf{X}|W}$ and Q_W . Using that $\mathbf{X} | W \sim N_d(\boldsymbol{\mu}, W\Sigma)$, it is easily verified that

$$\begin{aligned} Q_{\mathbf{X}|W}(\boldsymbol{\mu}, \Sigma^{-1}; \boldsymbol{\theta}_k) &= \sum_{i=1}^n \mathbb{E}(\log f_{\mathbf{X}|W}(\mathbf{X}_i | W_i; \boldsymbol{\mu}, \Sigma) | \mathbf{X}_i; \boldsymbol{\theta}_k) \\ &= -\frac{1}{2} \left(nd \log(2\pi) - n \log(\det(\Sigma^{-1})) + \sum_{i=1}^n (D^2(\mathbf{X}_i; \boldsymbol{\mu}, \Sigma) \delta_{ki} + d \xi_{ki}) \right). \end{aligned}$$

□

With $Q(\boldsymbol{\theta}; \boldsymbol{\theta}_k)$ at hand, we show in the following lemma how $\boldsymbol{\mu}$ and Σ are updated in Step 2.1) of Algorithm 5.1.

Lemma 5.3

Maximizing $Q(\boldsymbol{\theta}; \boldsymbol{\theta}_k)$ with respect to $\boldsymbol{\mu}$ and Σ in Step 2.1) of Algorithm 5.1 gives the next iterates

$$\boldsymbol{\mu}_{k+1} = \frac{\sum_{i=1}^n \delta_{ki} \mathbf{X}_i}{\sum_{i=1}^n \delta_{ki}} \quad \text{and} \quad \Sigma_{k+1} = \frac{1}{n} \sum_{i=1}^n \delta_{ki} (\mathbf{X}_i - \boldsymbol{\mu}_k)(\mathbf{X}_i - \boldsymbol{\mu}_k)^\top. \quad (22)$$

Proof. By Lemma 5.2, $Q(\boldsymbol{\theta}; \boldsymbol{\theta}_k) = Q_{\mathbf{X}|W}(\boldsymbol{\mu}, \Sigma^{-1}; \boldsymbol{\theta}_k) + Q_W(\boldsymbol{\nu}; \boldsymbol{\theta}_k)$ and $\boldsymbol{\mu}$ and Σ do not appear in $Q_W(\boldsymbol{\nu}; \boldsymbol{\theta}_k)$ so that we only need to maximize $Q_{\mathbf{X}|W}(\boldsymbol{\mu}, \Sigma^{-1}; \boldsymbol{\theta}_k)$.

The necessary conditions are given by $\frac{\partial}{\partial \boldsymbol{\mu}} Q_{\mathbf{X}|W}(\boldsymbol{\mu}, \Sigma^{-1}; \boldsymbol{\theta}_k) = 0$ and $\frac{\partial}{\partial \Sigma^{-1}} Q_{\mathbf{X}|W}(\boldsymbol{\mu}, \Sigma^{-1}; \boldsymbol{\theta}_k) = 0$. Using $\frac{\partial}{\partial \boldsymbol{\mu}} D^2(\mathbf{X}_i; \boldsymbol{\mu}, \Sigma) = -2\Sigma^{-1}(\mathbf{X}_i - \boldsymbol{\mu})$ one obtains that $\frac{\partial}{\partial \boldsymbol{\mu}} Q_{\mathbf{X}|W}(\boldsymbol{\mu}, \Sigma^{-1}; \boldsymbol{\theta}_k) = 0$ if and only if $\sum_{i=1}^n \delta_{ki} \Sigma^{-1}(\mathbf{X}_i - \boldsymbol{\mu}) = 0$. Solving for $\boldsymbol{\mu}$ gives $\boldsymbol{\mu}_{k+1}$ as given in the lemma. For full rank Σ , it holds that $\frac{\partial}{\partial \Sigma^{-1}} \log \det(\Sigma^{-1}) = \Sigma$. Since $\frac{\partial}{\partial \Sigma^{-1}} D^2(\mathbf{X}_i; \boldsymbol{\mu}, \Sigma) = (\mathbf{X}_i - \boldsymbol{\mu})(\mathbf{X}_i - \boldsymbol{\mu})^\top$ one gets $\frac{\partial}{\partial \Sigma^{-1}} Q_{\mathbf{X}|W}(\boldsymbol{\mu}, \Sigma^{-1}; \boldsymbol{\theta}_k) = 0$ if and only if $n\Sigma - \sum_{i=1}^n \delta_{ki} (\mathbf{X}_i - \boldsymbol{\mu})(\mathbf{X}_i - \boldsymbol{\mu})^\top = 0$ which, after solving for Σ , gives the formula for Σ_{k+1} as given in the statement. □

Lemma 5.3 indicates that we need to approximate the weights δ_{ki} , $i = 1, \dots, n$, in Step 2.1) of Algorithm 5.1. Note that

$$dF_{W|\mathbf{X}}(w | \mathbf{x}) = \frac{f_{\mathbf{X}|W}(\mathbf{x} | w) dF_W(w)}{f_{\mathbf{X}}(\mathbf{x})} = \frac{\phi(\mathbf{x}; \boldsymbol{\mu}, w\Sigma)}{f_{\mathbf{X}}(\mathbf{x})} dF_W(w), \quad w > 0,$$

where $\phi(\mathbf{x}; \boldsymbol{\mu}, \Sigma)$ denotes the density of $N_d(\boldsymbol{\mu}, \Sigma)$ so that

$$\begin{aligned} \delta_{ki} &= \mathbb{E} \left(\frac{1}{W_i} \middle| \mathbf{X}_i; \boldsymbol{\theta}_k \right) = \int_0^\infty \frac{1}{w} dF_{W|\mathbf{X}}(w | \mathbf{X}_i) \\ &= \frac{1}{f_{\mathbf{X}}(\mathbf{X}_i; \boldsymbol{\mu}_k, \Sigma_k, \boldsymbol{\nu}_k)} \int_0^\infty \frac{\phi(\mathbf{X}_i; \boldsymbol{\mu}_k, w\Sigma_k)}{w} dF_W(w; \boldsymbol{\nu}_k). \end{aligned}$$

This yields

$$\begin{aligned} \log(\delta_{ki}) &= \log \left(\int_0^\infty \frac{\phi(\mathbf{X}_i; \boldsymbol{\mu}_k, w\Sigma_k)}{w} dF_W(w; \boldsymbol{\nu}_k) \right) - \log f_{\mathbf{X}}(\mathbf{X}_i; \boldsymbol{\mu}_k, \Sigma_k, \boldsymbol{\nu}_k) \\ &= \log \left(\int_0^1 \frac{1}{\sqrt{(2\pi)^d F_W^{\leftarrow}(u; \boldsymbol{\nu}_k)^{d+2} |\Sigma_k|}} \exp \left(-\frac{D^2(\mathbf{X}_i; \boldsymbol{\mu}_k, \Sigma_k)}{2F_W^{\leftarrow}(u; \boldsymbol{\nu}_k)} \right) du \right) \\ &\quad - \log \left(\int_0^1 \frac{1}{\sqrt{(2\pi)^d F_W^{\leftarrow}(u; \boldsymbol{\nu}_k)^d |\Sigma_k|}} \exp \left(-\frac{D^2(\mathbf{X}_i; \boldsymbol{\mu}_k, \Sigma_k)}{2F_W^{\leftarrow}(u; \boldsymbol{\nu}_k)} \right) du \right). \end{aligned} \quad (23)$$

5 Fitting multivariate normal variance mixtures

Estimation of the latter integral (corresponding to $\log f_{\mathbf{X}}(\mathbf{x})$) was discussed in Algorithm 4.3; the former integral differs from the latter only by a factor of $F_W^{\leftarrow}(u)^{-1}$ can be estimated similarly; see Remark 4.4 for details.

Summarizing, the k 'th iteration of the algorithm consists of approximating the weights δ_{ki} , $i = 1, \dots, n$ with $\boldsymbol{\nu} = \boldsymbol{\nu}_k$ held fixed (which are then used to update $\boldsymbol{\mu}$ and Σ as in (22)) and then updating $\boldsymbol{\nu}$ by maximizing the original likelihood $\log L^{\text{org}}(\boldsymbol{\theta}; \mathbf{X}_1, \dots, \mathbf{X}_n)$ as a function of $\boldsymbol{\nu}$ with $\boldsymbol{\mu}$ and Σ set to their current estimates, i.e., we set

$$\boldsymbol{\nu}_{k+1} = \underset{\boldsymbol{\nu}}{\operatorname{argmax}} \log L^{\text{org}}(\boldsymbol{\nu}, \boldsymbol{\mu}_{k+1}, \Sigma_{k+1}; \mathbf{X}_1, \dots, \mathbf{X}_n) \quad (24)$$

and solve this p_{ν} -dimensional optimization problem numerically. In most settings, the dimension p_{ν} of $\boldsymbol{\nu}$ is small so that this optimization problem is numerically feasible. This step is the most costly one as it involves multiple estimation of the likelihood of the data using Algorithm 4.3: Each call to the likelihood function requires the approximation of n integrals. It turns out that estimating the weights δ_{ki} is faster so that it seems to be fruitful to first update $\boldsymbol{\mu}$ and Σ until convergence (with $\boldsymbol{\nu} = \boldsymbol{\nu}_k$ held fixed) and then update $\boldsymbol{\nu}$. In fact, this can be done efficiently: The weights δ_{ki} depend on \mathbf{X}_i , $\boldsymbol{\mu}_k$ and Σ_k only through the Mahalanobis distances $D^2(\mathbf{X}_i; \boldsymbol{\mu}_k, \Sigma_k)$. Once $\boldsymbol{\mu}_k$ and Σ_k are updated to, say, $\boldsymbol{\mu}'_k$ and Σ'_k , (some of) the new weights δ'_{ki} for the new Mahalanobis distances $D^2(\mathbf{X}_i; \boldsymbol{\mu}'_k, \Sigma'_k)$ can be obtained by interpolating the already calculated weights δ_{ki} corresponding to the (old) Mahalanobis distances $D^2(\mathbf{X}_i; \boldsymbol{\mu}_k, \Sigma_k)$.

It remains to discuss how a starting value $\boldsymbol{\theta}_0$ can be found. We suggest using $\boldsymbol{\mu}_0 = \bar{\mathbf{X}}_n$, the sample mean vector, as unbiased estimator for $\boldsymbol{\mu}$. Denote by S_n the sample covariance matrix (Wishart matrix) of $\mathbf{X}_1, \dots, \mathbf{X}_n$. Since S_n is unbiased for $\operatorname{cov}(\mathbf{X})$ it follows that $\mathbb{E}(S_n) = \mathbb{E}(W)\Sigma$. The idea is now to maximize the likelihood given $\boldsymbol{\mu} = \boldsymbol{\mu}_0$ and given $\Sigma = c \cdot S_n$ with respect to $\boldsymbol{\nu}$ and c (restricted to $c > 0$) which is a $(p_{\nu} + 1)$ dimensional optimization problem. That is, we find

$$(\boldsymbol{\nu}^*, c^*) = \underset{\boldsymbol{\nu}, c > 0}{\operatorname{argmax}} L^{\text{org}}(\boldsymbol{\nu}, \boldsymbol{\mu}_0, cS_n; \mathbf{X}_1, \dots, \mathbf{X}_n) \quad (25)$$

numerically and set $\boldsymbol{\nu}_0 = \boldsymbol{\nu}^*$ and $\Sigma_0 = c^* S_n$ which is just a multiple of the Wishart matrix.

The complete procedure is summarized in Algorithm 5.4. As convergence criterion we suggest stopping once the maximal relative difference in parameter estimates is smaller than a given threshold. We define the maximal relative difference by

$$d(\boldsymbol{\nu}_k, \boldsymbol{\nu}_{k+1}) = \max_{i=1, \dots, d} \frac{|\nu_{k,i} - \nu_{k+1,i}|}{|\nu_{k,i}|}, \quad \boldsymbol{\nu}_k = (\nu_{k,1}, \dots, \nu_{k,p_{\nu}})$$

and similarly for $\boldsymbol{\mu}$ and Σ .

Algorithm 5.4 (ECME algorithm for fitting normal variance mixtures)

Given iid input data $\mathbf{X}_1, \dots, \mathbf{X}_n$ and convergence criteria $\varepsilon_{\boldsymbol{\mu}}$, ε_{Σ} and $\varepsilon_{\boldsymbol{\nu}}$, estimate $\boldsymbol{\mu}$, Σ , $\boldsymbol{\nu}$ via:

6 Gamma Mixture Models

1) Starting value.

Set $\boldsymbol{\mu}_0 = \bar{\mathbf{X}}_n$ and solve the optimization problem (25) numerically to obtain $\boldsymbol{\nu}^*$ and c^* .
Set $\boldsymbol{\nu}_0 = \boldsymbol{\nu}^*$ and $\Sigma_0 = c^* S_n$.

2) ECME iteration.

For $k = 0, 1, \dots$, do:

2.1) Update $\boldsymbol{\mu}$ and Σ .

Set $\boldsymbol{\mu}_k^{(1)} = \boldsymbol{\mu}_k$ and $\Sigma_k^{(1)} = \Sigma_k$.

For $l = 1, \dots$, do:

2.1.1) Estimate new weights $\delta_{ki}^{(l+1)} = \mathbb{E}(1/W_i \mid \mathbf{X}_i; \boldsymbol{\mu}_k^{(l)}, \Sigma_k^{(l)}, \boldsymbol{\nu}_k)$, $i = 1, \dots, n$ using (23) and Algorithm 4.3.

2.1.2) Calculate the new iterates $\boldsymbol{\mu}_k^{(l+1)}$ and $\Sigma_k^{(l+1)}$ using (22) with weights $\delta_{ki}^{(l+1)}$, $i = 1, \dots, n$.

2.1.3) If $d(\boldsymbol{\mu}_k^{(l)}, \boldsymbol{\mu}_k^{(l+1)}) < \varepsilon_\mu$ and $d(\Sigma_k^{(l)}, \Sigma_k^{(l+1)}) < \varepsilon_\Sigma$, set $\boldsymbol{\mu}_{k+1} = \boldsymbol{\mu}_k^{(l+1)}$, $\Sigma_{k+1} = \Sigma_k^{(l+1)}$ and go to Step 2.2).

2.2) Update $\boldsymbol{\nu}$.

Numerically solve the optimization problem (24) to obtain $\boldsymbol{\nu}_{k+1}$.

2.3) If $d(\boldsymbol{\nu}_k, \boldsymbol{\nu}_{k+1}) < \varepsilon_\nu$, return the MLEs $\boldsymbol{\mu}^* = \boldsymbol{\mu}_{k+1}$, $\Sigma^* = \Sigma_{k+1}$ and $\boldsymbol{\nu}^* = \boldsymbol{\nu}_{k+1}$.

6 Gamma Mixture Models

For statistical purposes it is often interesting to study the distribution of the squared Mahalanobis distance of $\mathbf{X} \sim \text{NVM}_d(\boldsymbol{\mu}, \Sigma, F_W)$ given by $D^2(\mathbf{X}; \boldsymbol{\mu}, \Sigma) = (\mathbf{X} - \boldsymbol{\mu})^\top \Sigma^{-1}(\mathbf{X} - \boldsymbol{\mu})$. We write $D^2 := D^2(\mathbf{X}; \boldsymbol{\mu}, \Sigma)$ if there is no confusion.

It follows readily from the stochastic representation (1) of \mathbf{X} that, in distribution,

$$D^2 = W X^2$$

where $X^2 \sim \chi_d^2$. This immediately gives rise to a sampling algorithm to generate random variates from D^2 . Since a χ^2 distribution is a special case of a gamma distribution, it follows that $D^2 \mid W \sim \Gamma(d/2, 2W)$ where $\Gamma(\alpha, \beta)$ denotes a gamma distribution with shape $\alpha > 0$ and scale $\beta > 0$ which admits the density $f_{\Gamma(\alpha, \beta)}(x) = (\Gamma(\alpha)\beta^\alpha)^{-1} x^{\alpha-1} e^{-x/\beta}$, $x > 0$, and distribution function $F_{\Gamma(\alpha, \beta)}(x) = \int_0^x f_{\Gamma(\alpha, \beta)}(t) dt$ for $x > 0$. The function $\Gamma(z) = \int_0^\infty t^{z-1} e^{-t} dt$, $z > 0$ denotes the gamma function.

In the special case where $W = 1$ almost surely, $D^2 \sim \chi_d^2$; if W follows an inverse-gamma distribution so that \mathbf{X} follows a multivariate t with $\nu > 0$ degrees of freedom, it can be easily seen that $D^2/d \sim F(d, \nu)$. For the general case where only F_W^\leftarrow is available, we can use methods similar to the ones developed so far to approximate the density and the distribution function of D^2 .

6 Gamma Mixture Models

Estimating the distribution function of D^2 . Using a conditioning argument similar to the normal variance mixture case, we obtain that

$$F_{D^2}(x) = \mathbb{P}(D^2 \leq x) = \mathbb{E} \left(F_{\Gamma(d/2, 2)} \left(\frac{x}{W} \right) \right), \quad x \geq 0.$$

This univariate integral can be approximated directly using an RQMC approach similar to Algorithm 3.1. An implementation can be found in the function `pgammamix()` in the R package `nvmmix`.

Estimating the density function of D^2 . In a similar fashion as in the derivation of Equation (3), the density of D^2 can be calculated as $f_{D^2}(x) = \int_0^1 \tilde{h}(u) du$ for $x > 0$, where

$$\tilde{h}(u) = \frac{1}{\Gamma(d/2)(2F_W^{\leftarrow}(u))^{d/2}} x^{d/2-1} \exp \left(-\frac{x}{2F_W^{\leftarrow}(u)} \right), \quad u \in (0, 1).$$

The functions \tilde{h} and h from Equation (16) differ only in constants with respect to u , the functional form is identical. Algorithm 4.3 can then, with some slight modifications, be used to estimate the density $f_{D^2}(x)$ (or $\log f_{D^2}(x)$). This is implemented in the function `dgammamix()` in the R package `nvmmix`.

Estimating the quantile function of D^2 . For many applications, such as graphical goodness-of-fit testing or random variate generation, it is useful to have the quantile function of D^2 available. Note that both the density and the distribution function of D^2 can be estimated as discussed above; the quantile function can then be estimated by numerically solving the equation $F_{D^2}(q_u) - u = 0$ for q_u where $u \in (0, 1)$ is given. We suggest using Newton's method: In iteration $k \geq 1$, given a current iterate $q_u^{(k)}$, the next iterate is given by

$$\begin{aligned} q_u^{(k+1)} &= q_u^{(k)} - \frac{F_{D^2}(q_u^{(k)}) - u}{f_{D^2}(q_u^{(k)})} \\ &= q_u^{(k)} - \text{sign}(F_{D^2}(q_u^{(k)}) - u) \exp \left\{ \log \left(|F_{D^2}(q_u^{(k)}) - u| \right) - \log f_{D^2}(q_u^{(k)}) \right\}. \end{aligned}$$

The second line is a numerically more stable version of the first. We remark that (potentially) many calls to $F_{D^2}(\cdot)$ and $f_{D^2}(\cdot)$ are necessary until convergence takes place. We also note that in most applications, the quantile function has to be evaluated at multiple inputs, say u_1, \dots, u_n . In order to reduce run time, one can sort the inputs u_i in increasing order and also store all calls to $F_{D^2}(\cdot)$ and $f_{D^2}(\cdot)$. These values can be used as starting values for the next quantile calculation. If they are reasonably close to the true quantile, the procedure enjoys local quadratic convergence so that only a few calls to $F_{D^2}(\cdot)$ and $f_{D^2}(\cdot)$ are needed. Furthermore, $F_{D^2}(\cdot)$ and $f_{D^2}(\cdot)$ can be estimated simultaneously using the same realizations of W , and all those realizations can also be stored so that they do not need to

be generated more often than necessary. This is implemented in the function `qgammamix()` in the R package `nvmmix`; the same idea can be exploited to estimate the quantile function of univariate normal variance mixtures which is implemented in the function `qnvmmix()`.

7 Numerical Examples

In this section we provide a careful numerical analysis of all algorithms presented. The first part discusses the type of mixing distributions used; the second, third and fourth part detail numerical examples for estimating the distribution function using Algorithm 3.1 with variable reordering as in Algorithm 3.2, estimating the log-density function using Algorithm 4.3 and estimating parameters ν , $\boldsymbol{\mu}$ and Σ given a random sample using Algorithm 5.4, respectively. The last part provides an application of our methods to a multivariate financial data set.

7.1 Test Distributions

For our numerical examples, we consider two distributions for the mixing variable W , an inverse-gamma distribution (so that \mathbf{X} is multivariate t) and a Pareto distribution.

Inverse-gamma mixture. Here W follows an inverse-gamma distribution with shape and rate parameter $\nu/2$. The resulting distribution is the multivariate t distribution, $\mathbf{X} \sim \text{MVT}_d(\nu, \boldsymbol{\mu}, \Sigma)$ with positive degrees of freedom ν . Note that if $\nu > 1$, $\mathbb{E}(\mathbf{X}) = \boldsymbol{\mu}$ and if $\nu > 2$, $\text{cov}(\mathbf{X}) = \frac{\nu}{\nu-2}\Sigma$. The multivariate t distribution has the density

$$f_{\mathbf{X}}(\mathbf{x}) = \frac{\Gamma((\nu + d)/2)}{\Gamma(\nu/2)\sqrt{(\nu\pi)^d|\Sigma|}} \left(1 + D^2(\mathbf{x}; \boldsymbol{\mu}, \Sigma)\right)^{-\frac{\nu+d}{2}}, \quad \mathbf{x} \in \mathbb{R}^d. \quad (26)$$

For the ECME procedure it is useful to calculate the weight $\mathbb{E}(1/W \mid \mathbf{X})$. Since

$$f_{W|\mathbf{X}}(w \mid \mathbf{x}) \propto f_{\mathbf{X}|W}(\mathbf{x} \mid w)f_W(w) \propto w^{-\frac{d+\nu}{2}-1} \exp\left(-\frac{(D^2(\mathbf{x}; \boldsymbol{\mu}, \Sigma) + \nu)/2}{w}\right), \quad w > 0,$$

$W \mid \mathbf{X}$ follows an inverse-gamma distribution, i.e., $W \mid \mathbf{X} \sim \text{IG}((d + \nu)/2, (D^2(\mathbf{X}; \boldsymbol{\mu}, \Sigma) + \nu)/2)$. This implies

$$\mathbb{E}(1/W \mid \mathbf{X}) = \frac{\nu + d}{\nu + D^2(\mathbf{X}; \boldsymbol{\mu}, \Sigma)},$$

so that the weights δ_{ki} in Step 2.1.1) of Algorithm 5.4 can be calculated analytically in this case.

Pareto mixture.

In order to test our algorithms for a normal variance mixture distribution that has not been

7 Numerical Examples

studied as extensively as the multivariate t distribution we consider $W \sim \text{Par}(\alpha, x_m)$ with density

$$f_W(w) = \alpha \frac{x_m^\alpha}{w^{\alpha+1}}, \quad w \geq x_m.$$

One can calculate that $\mathbb{E}(W^k)$ exists with $\mathbb{E}(W^k) = \alpha/(\alpha - k)$ if $k < \alpha$. This implies for the resulting normal variance mixture $\mathbf{X} = \boldsymbol{\mu} + \sqrt{W}\mathbf{A}\mathbf{Z}$ that $\mathbb{E}(\mathbf{X}) = \boldsymbol{\mu}$ for $\alpha > 1/2$ and $\text{cov}(\mathbf{X}) = \frac{\alpha}{\alpha-1}\Sigma$ for $\alpha > 1$. The density $f_{\mathbf{X}}(\mathbf{x}) = f_{\mathbf{X}}(\mathbf{x}; \boldsymbol{\mu}, \Sigma, \alpha, x_m)$ can be determined using (4):

$$\begin{aligned} f_{\mathbf{X}}(\mathbf{x}) &= \frac{\alpha x_m^\alpha}{\sqrt{(2\pi)^d |\Sigma|}} \int_{x_m}^{\infty} w^{-d/2-\alpha-1} \exp\left(-\frac{D^2(\mathbf{x}; \boldsymbol{\mu}, \Sigma)}{2w}\right) dw \\ &= \frac{\alpha x_m^\alpha}{\sqrt{(2\pi)^d |\Sigma|}} \left(\frac{D^2(\mathbf{x}; \boldsymbol{\mu}, \Sigma)}{2}\right)^{-d/2-\alpha} \int_0^{\frac{D^2(\mathbf{x}; \boldsymbol{\mu}, \Sigma)}{2x_m}} u^{d/2+\alpha-1} \exp(-u) du \\ &= \frac{\alpha x_m^\alpha}{\sqrt{(2\pi)^d |\Sigma|}} \left(\frac{D^2(\mathbf{x}; \boldsymbol{\mu}, \Sigma)}{2}\right)^{-d/2-\alpha} \gamma\left(\alpha + \frac{d}{2}; \frac{D^2(\mathbf{x}; \boldsymbol{\mu}, \Sigma)}{2x_m}\right), \quad \mathbf{x} \in \mathbb{R}^d, \end{aligned}$$

where $\gamma(z; x) = \int_0^x t^{z-1} e^{-t} dt$ for $z, x > 0$ denotes the (lower) incomplete gamma function. Note that $f_{\mathbf{X}}(\mathbf{x}; \boldsymbol{\mu}, \Sigma, \alpha, x_m) = f_{\mathbf{X}}(\mathbf{x}; \boldsymbol{\mu}, x_m \Sigma, \alpha, 1)$ so that the scale parameter x_m is redundant as the scaling can be achieved via scaling Σ . We can thus set $x_m = 1$ and obtain

$$f_{\mathbf{X}}(\mathbf{x}; \boldsymbol{\mu}, \Sigma, \alpha) = \frac{\alpha}{\sqrt{(2\pi)^d |\Sigma|}} \left(\frac{D^2(\mathbf{x}; \boldsymbol{\mu}, \Sigma)}{2}\right)^{-d/2-\alpha} \gamma\left(\alpha + \frac{d}{2}; \frac{D^2(\mathbf{x}; \boldsymbol{\mu}, \Sigma)}{2}\right), \quad \mathbf{x} \in \mathbb{R}^d. \quad (27)$$

We use the notation $\mathbf{X} \sim \text{PNVM}(\alpha, \boldsymbol{\mu}, \Sigma)$ (“Pareto normal variance mixture”) for a random vector \mathbf{X} with density (27).

As in the case of an inverse-gamma mixture, it is possible to derive an expression for $\mathbb{E}(1/W \mid \mathbf{X})$ in the Pareto setting. Note that

$$f_{W|\mathbf{X}}(w \mid \mathbf{x}) \propto f_{\mathbf{X}|W}(\mathbf{x} \mid w) f_W(w) \propto w^{-(\alpha+d/2+1)} \exp\left(-D^2(\mathbf{x}; \boldsymbol{\mu}, \Sigma)/2\right), \quad w > 1,$$

so that using the density transformation formula we obtain for $\tilde{W} = 1/W$ that

$$f_{\tilde{W}|\mathbf{X}}(\tilde{w} \mid \mathbf{x}) \propto \tilde{w}^{\alpha+d/2-1} \exp(-\tilde{w} D^2(\mathbf{x}; \boldsymbol{\mu}, \Sigma)/2), \quad \tilde{w} \in (0, 1).$$

Therefore, $W^{-1} \mid \mathbf{X}$ follows a $(0, 1)$ truncated gamma distribution with shape $\alpha + d/2$ and scale $2/D^2(\mathbf{X}; \boldsymbol{\mu}, \Sigma)$. For more details on truncated gamma distributions, see Coffey and Muller (2000); Equation (2.12) therein implies that

$$\mathbb{E}(1/W \mid \mathbf{X}) = \frac{F_{\Gamma}(1; \alpha + d/2 + 1, 2/D^2(\mathbf{X}; \boldsymbol{\mu}, \Sigma))}{F_{\Gamma}(1; \alpha + d/2, 2/D^2(\mathbf{X}; \boldsymbol{\mu}, \Sigma))} \frac{2\alpha + d}{D^2(\mathbf{X}; \boldsymbol{\mu}, \Sigma)}.$$

7.2 Estimating the distribution function

In the case where $\mathbf{X} \sim \text{MVT}_d(\nu, \boldsymbol{\mu}, \Sigma)$, Algorithm 3.1 combined with the variable reordering Algorithm 3.2, implemented in the function `pStudent()` in the R package `nvmmix` is similar to the one developed in Genz and Bretz (2002) (therein referred to as QRSVN algorithm) which is implemented in the function `pmvt()` of the R package `mvtnorm` (Genz, Bretz, et al. (2019)). The main difference between our algorithm and the QRSVN algorithm lies in the choice of quasi-random numbers: The QRSVN algorithm uses randomized Korobov rules (which belong to the wider class of lattice rules; see Keast (1973) and Cranley and Patterson (1976)) whereas we use a Sobol' sequence (which is a digital net). Furthermore, our implementation relies on C code, whereas `pmvt()` internally calls Fortran code.

7.2.1 Error behaviour as a function of the sample size

In order to assess the performance of our algorithm let us first consider estimated absolute errors as a function of the number of function evaluations. Four settings are considered: (pure) MC with and without reordering and RQMC (using a randomized Sobol' sequence) with and without reordering. In Figures 2 and 3, estimated absolute errors (estimated as in Algorithm 3.1 via $\hat{\varepsilon}$ in Step 4.3)) are reported for different sample sizes n (which refer to the total number of function evaluations) in different dimensions using the four aforementioned methods for the multivariate t case and the Pareto mixture. For each dimension and for each n we report the average estimated absolute error for 15 different parameter settings. In each parameter setting, an upper limit is randomly chosen via $\mathbf{b} \sim \text{U}(0, 3\sqrt{d})^d$ and a correlation matrix R is sampled as a random Wishart matrix via the function `rWishart()` in R. The lower limit is set to $\mathbf{a} = (-\infty, \dots, -\infty)$. The degrees of freedom ν in the MVT setting and the shape parameter α in the PNVM setting are set to 2.

It is evident that RQMC methods yield lower errors than their MC counterparts. We also report the convergence speed (as measured by the regression coefficient α of $\log \hat{\varepsilon} = \alpha \log n + c$ displayed in the legend): Variable reordering does not have an influence on the convergence speed $1/\sqrt{n}$ of MC methods; however, it does speed up the RQMC methods. A possible explanation is that variable reordering can reduce the effective dimension. This is discussed below in more detail.

7.2.2 The effect of variable reordering

Investigating the variance of the integrand. It is interesting to further investigate the effect of variable reordering as detailed in Section 3.3. To this end, the variance of the integrand g from (12) given by

$$\text{var}(g(\mathbf{U})) = \int_{[0,1]^d} g^2(\mathbf{u}) d\mathbf{u} - \left(\int_{[0,1]^d} g(\mathbf{u}) d\mathbf{u} \right)^2$$

is estimated, once with the original g without reordering, and once with \tilde{g} which is the integrand g after applying Algorithm 3.2 to the inputs $\mathbf{a}, \mathbf{b}, \Sigma$. We use a randomized

7 Numerical Examples

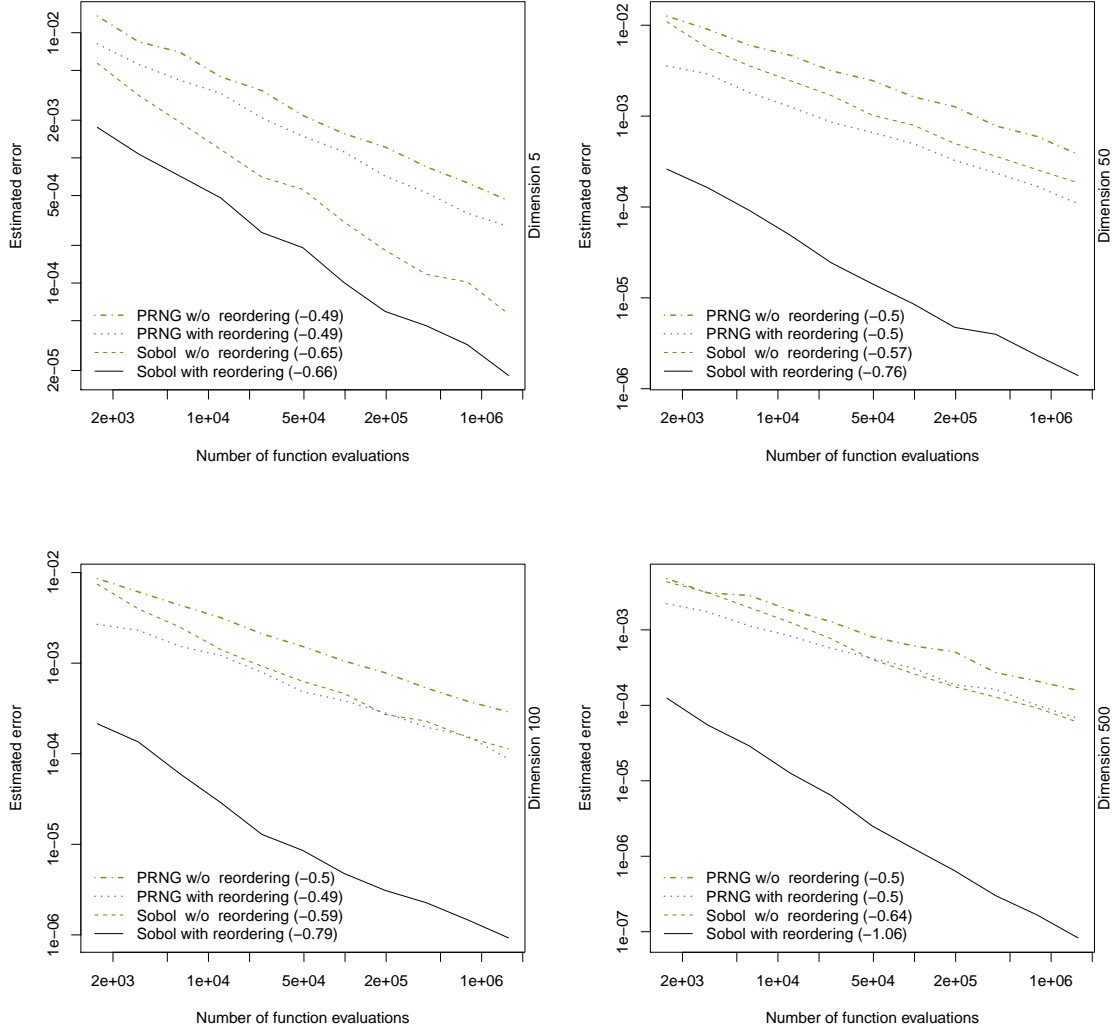


Figure 2 Average absolute errors of different estimators for $F_{\mathbf{X}}(\mathbf{x})$ as a function of n for $\mathbf{X} \sim \text{MVT}_d(2, \mathbf{0}, \Sigma)$, where for each n , 15 different settings for Σ and \mathbf{x} are randomly chosen. Regression coefficients are in parentheses in the legends.

experiment and do the following 50 000 times for an inverse-gamma mixture: Sample $d \sim U(\{5, \dots, 500\})$, $\nu \sim U(0.1, 5)$ and \mathbf{a} , \mathbf{b} , Σ are randomly chosen as in the previous section. The variance of the integrand is then estimated via the sample variance of $g(\mathbf{U}_1), \dots, g(\mathbf{U}_N)$ for $N = 10\,000$. Results can be found in Figure 4: On the left, variances have been ordered according to the ordering of the variances when variable reordering is

7 Numerical Examples

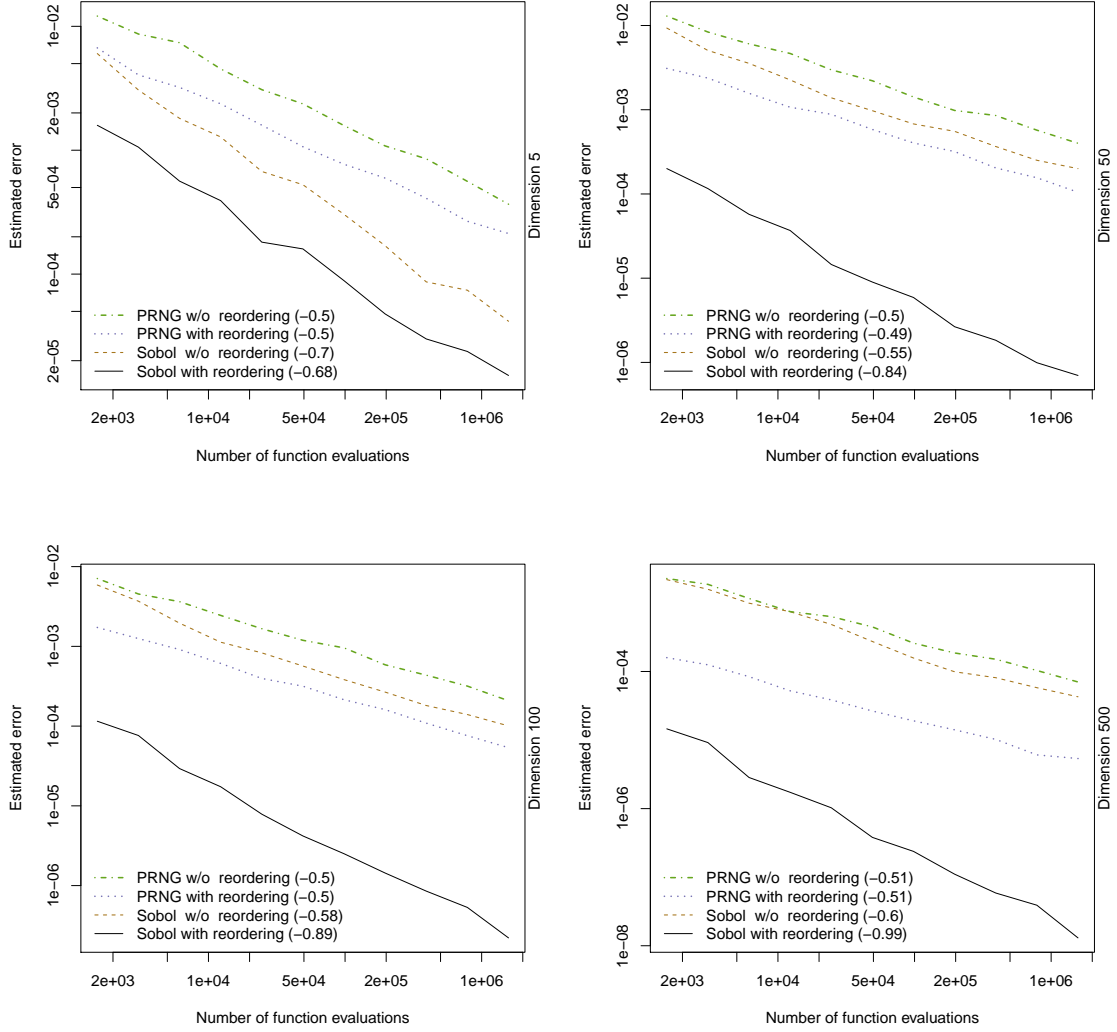


Figure 3 Average absolute errors of different estimators for $F_{\mathbf{X}}(\mathbf{x})$ as a function of n for $\mathbf{X} \sim \text{PNVM}_d(2, \mathbf{0}, \Sigma)$, where for each n , 15 different settings for Σ and \mathbf{x} are randomly chosen. Regression coefficients are in parentheses in the legends.

employed (for better visibility of the reordering effect). On the right, a density plot of the ratios $\text{var}(\tilde{g}(\mathbf{U})) / \text{var}(g(\mathbf{U}))$ is shown. It can be confirmed that in the vast majority of cases, variable reordering substantially decreases the variance of the integrand. In only 12 of the 50 000 runs did the estimated variance after reordering exceed the variance without reordering.

7 Numerical Examples

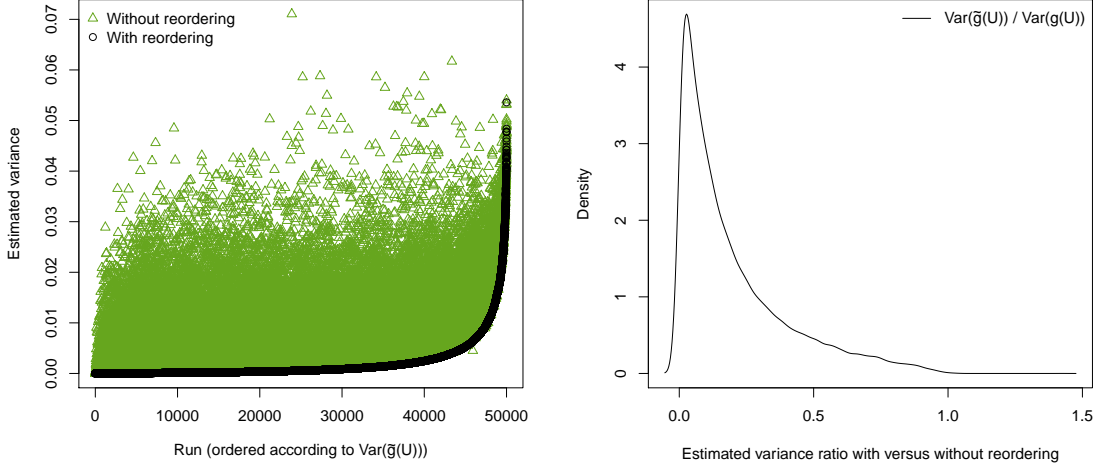


Figure 4 Left: Variance of the integrand $\text{var}(g(\mathbf{U}))$ with and without variable reordering. Right: Histogram of estimated variance ratios. Ratios larger than 30 were set to 30.

Effective dimension of the integrand. As was seen in Figures 2 and 3, reordering improves both MC and RQMC methods; the effect is however stronger for RQMC methods. A possible explanation for this is that the variable reordering not only reduces the overall variance of the integrand, $\sigma^2 = \text{var}(g(\mathbf{U}))$ as seen in the previous part, but also the *effective dimension* of the integrand, to be defined later. (R)QMC methods often work better if only a small number of variables are important, see Wang and Fang (2003) and references therein for a discussion and examples. Variable reordering as explained in Section 3.3 was derived in a way such that the first components are the most important ones, see also Remark 3.3.

Sensitivity indices, such as Sobol' indices, can help understand the importance of different variables of an integrand. Following Lemieux (2009, Ch. 6.3) and Sobol' (2001), we consider the ANOVA decomposition of a (square integrable) function $g : (0, 1)^d \rightarrow \mathbb{R}$ given by

$$g(\mathbf{u}) = \sum_{I \subseteq \{1, \dots, d\}} g_I(\mathbf{u})$$

where

$$g_I(\mathbf{u}) = \int_{[0,1]^{d-k}} g(\mathbf{u}) d\mathbf{u}_{-I} - \sum_{J \subset I} g_J(\mathbf{u}), \quad g_\emptyset(\mathbf{u}) = \int_{[0,1]^d} g(\mathbf{u}) d\mathbf{u};$$

here, $k = |I|$ and \mathbf{u}_{-I} is the vector \mathbf{u} without components $k \in I$. The g_I 's only depend on variables $i \in I$ and are orthogonal; if $I \neq \emptyset$, g_I has mean zero. The overall variance of the

7 Numerical Examples

integrand can then be decomposed as

$$\sigma^2 = \text{var}(g(\mathbf{U})) = \sum_{I \subseteq \{1, \dots, d\}} \sigma_I^2$$

where $\sigma_I^2 = \text{var}(g_I(\mathbf{U})) = \int_{[0,1]^d} g_I(\mathbf{u})^2 d\mathbf{u}$. The number

$$S_I = \frac{\sigma_I^2}{\sigma^2} \in [0, 1]$$

is called *Sobol' index* of I . It explains the fraction of the overall variance of the integrand explained by the variables in I ; if this number is close to 1, it means that most of the variance is explained by g_I and therefore by the variables in I . If $I = \{l\}$ is a singleton $S_I = S_l$ is called a *first order index*.

Another useful sensitivity index is the *total effect index* of variable $l \in \{1, \dots, d\}$ given by

$$S_{T_l} = \frac{1}{\sigma^2} \sum_{I \subseteq \{1, \dots, d\}: l \in I} \sigma_I^2$$

which measures the relative impact of component l and all its interactions. Care must be taken when interpreting this value as $\sum_{i=1}^d S_{T_i} \geq 1$ in general since interactions are counted several times. For instance, $\sigma_{\{1,2\}}^2$ is contained in S_{T_1} as well as in S_{T_2} .

Finally, the *effective dimension in the superposition sense* in proportion $p \in (0, 1]$ is the smallest integer d_S so that

$$\frac{1}{\sigma^2} \sum_{I: |I| \leq d_S} \sigma_I^2 \geq p.$$

If the effective dimension is d_S , the integrand can be well approximated by functions of at most d_S variables; see Lemieux (2009, Sec. 3.6.1).

The indices $S_{\{l\}}$ and S_{T_l} for $l \in \{1, \dots, d\}$ can be estimated using Owen (2013)'s method which is implemented in the function `sobolowen()` in the R package `sensitivity`; see Pujol et al. (2017). Figure 5 shows estimated Sobol' indices in two settings: In each setting, $W \sim \text{IG}(1/2, 1/2)$ (so that \mathbf{X} follows a multivariate t distribution with 1 degrees of freedom) and $d = 10$. The upper limit \mathbf{b} and the scale matrix Σ were found by trial & error so that there is either a substantial variance reduction (top figure) achieved by reordering or an increase in variance (bottom figure). In order to be consistent with the definition of the integrand g in (12), variables are called $0, \dots, d-1$ so that they correspond to u_0, \dots, u_{d-1} . For instance, in the top figure, one can read that $S_{(0)} \approx 0.52$ after reordering so that 52% of the variance of g can be explained by a function $g_{\{0\}}(u_0)$.

Inspecting the top figures where variable reordering led to a decrease in variance of approximately 99% reveals that both first order and total effect indices are decreasing in the dimension after variable reordering was performed. Also, the figure label includes the sum of the first order indices. After reordering, 65% (as opposed to 15%) of the overall variance of the integrand is explained by components g_I of g of exactly one variable, hinting at the

7 Numerical Examples

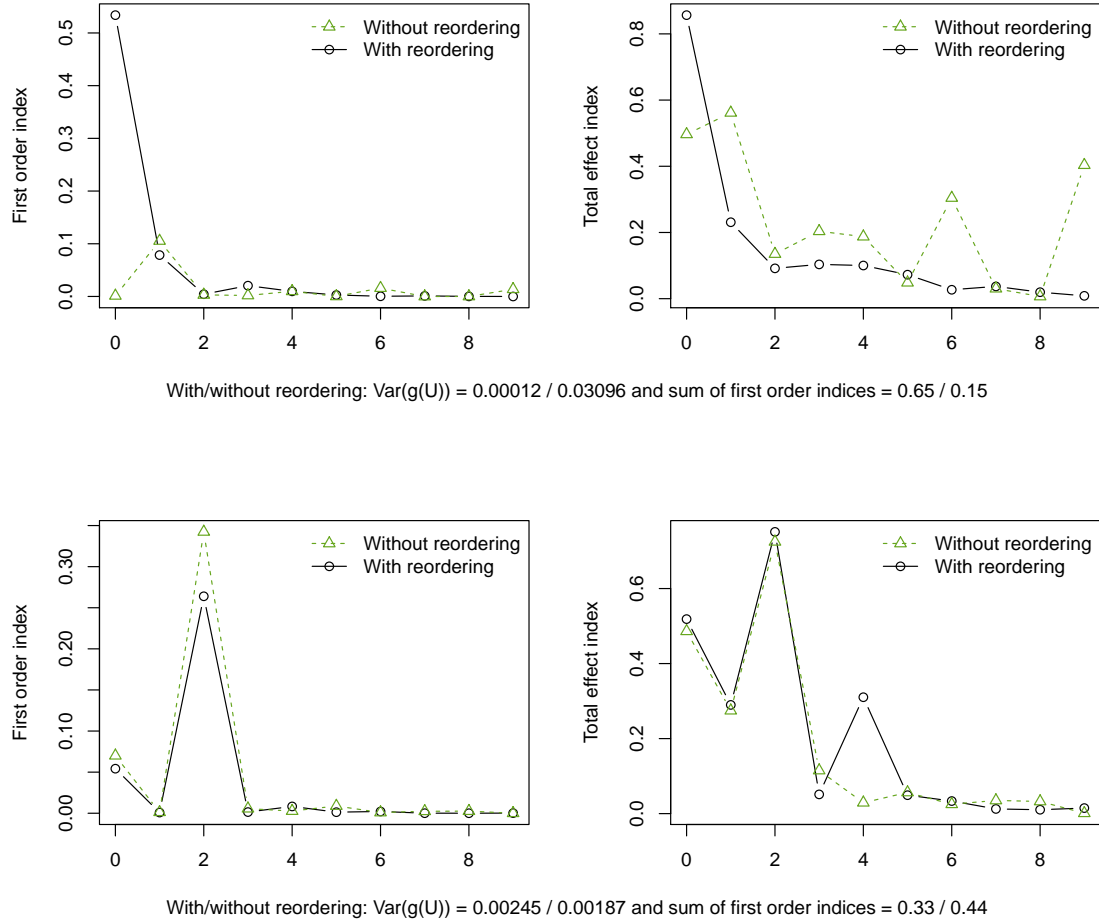


Figure 5 Estimated first order and total effect indices with and without reordering for an inverse-gamma mixture in a setting with high variance reduction (top) and increase in variance (bottom).

fact that the effective dimension decreased: The effective dimension in the superposition sense in proportion 65% decreased to 1 after reordering.

There are rare cases when variable reordering leads to an increase in variance: In the bottom figures, the relative increase is about 31%. Here, the new ordering is clearly not optimal and indices are not decreasing with the dimension. Given the nature of the greedy procedure it is expected that in some cases, no improvement is achieved.

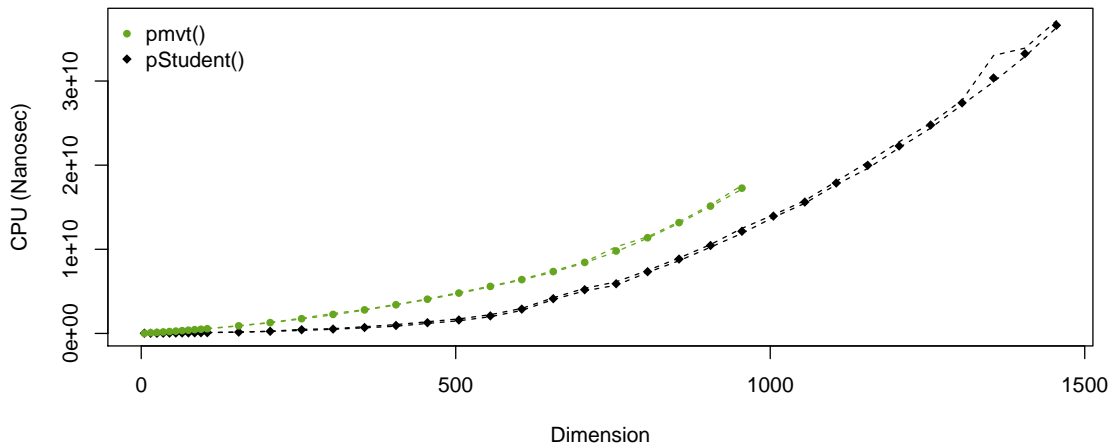


Figure 6 Run times based on three replications of 15 randomly chosen inputs \mathbf{b} and Σ in each dimension.

7.2.3 Run times

In this part we take a brief look at the run-times of Algorithm 3.1 combined with the variable reordering Algorithm 3.2. We restrict our attention to the important multivariate t case and compare run times of our implementation in `pStudent()` with the run times of the above mentioned QRSVN algorithm described in Genz and Bretz (2002) and provided by the function `pmvt()` in the R package `mvtnorm`.

In order to get meaningful estimates of the CPU time, for each dimension d , the following is done 15 times: Sample \mathbf{b} and Σ as before when estimating $\text{var}(g(\mathbf{U}))$, set $\mathbf{a} = (-\infty, \dots, -\infty)$ and $\nu = 2$. Then call `pmvt()` and `pStudent()` three times each and average their CPU times obtained using the package `microbenchmark` of Mersmann (2015). The above procedure is done for an absolute error tolerance $\varepsilon = 0.001$ and the maximum number of function evaluations is chosen such that both algorithms always terminate with the correct precision.

Figure 6 shows the run times obtained. The symbols represent the corresponding means whereas the lines show the largest/smallest CPU time measured for that dimension. Note that `pmvt()` only works for dimensions up to 1000. Figure 6 shows that our implementation is competitive with the current standard.

7.3 Estimating the density function

In this section we test the performance of Algorithm 4.3 to estimate the log-density of $\mathbf{X} \sim \text{MVT}_d(\nu, \boldsymbol{\mu}, \Sigma)$ and $\mathbf{X} \sim \text{PNVM}_d(\alpha, \boldsymbol{\mu}, \Sigma)$. Note that the density is known in either

7 Numerical Examples

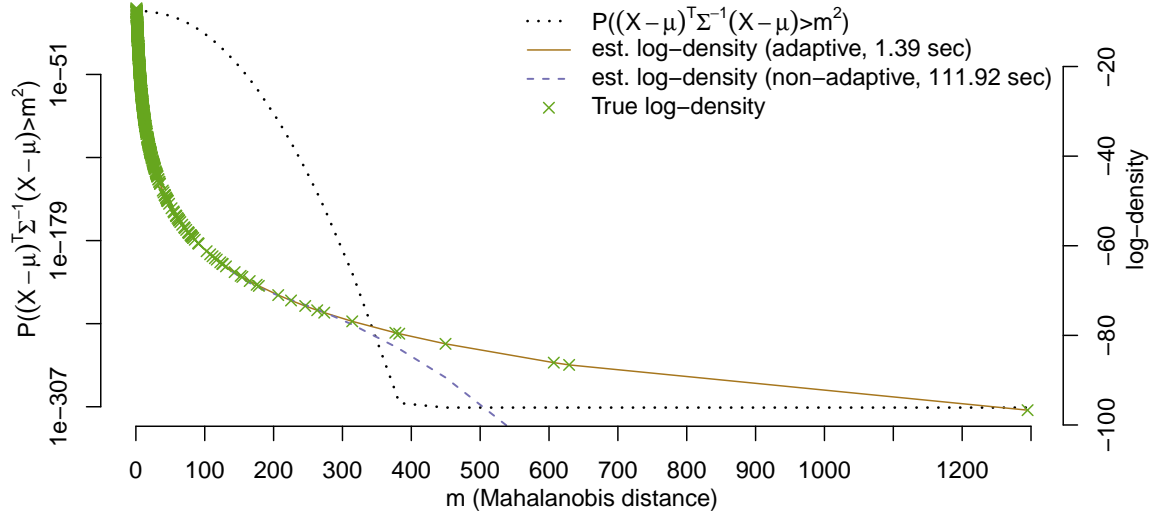


Figure 7 Estimated log-density of $\text{MVT}_d(\nu = 4, \mathbf{0}, I_d)$ in $d = 10$ evaluated at $n = 1000$ points sampled from $\text{MVT}_d(\nu = 1, \mathbf{0}, I_d)$.

case and given in (26) and (27) so that estimated and true log-density values can be compared.

We sample $n = 1000$ points from $\mathbf{X} \sim \text{MVT}_d(\nu = 1, \mathbf{0}, I_d)$ in dimension $d = 10$ and evaluate the density of $\text{MVT}_d(\nu = 4, \mathbf{0}, I_d)$ at the sampled points. The Pareto case is done similarly.

Figures 7 and 8 display results obtained by the adaptive algorithm (Algorithm 4.3) and by the crude (non-adaptive) algorithm (Algorithm 4.1); the true log-density and the probability $\mathbb{P}(D^2(\mathbf{X}, \mathbf{0}, I_d) > m^2)$ are also plotted. The latter probability gives an idea of how likely it is to see a sample point \mathbf{x} with Mahalanobis distance greater than m . For small Mahalanobis distances, both algorithms perform well. For larger ones the problem becomes harder as the underlying integrand becomes more difficult to integrate (recall Figure 1 and the discussion thereafter) and the crude, non-adaptive version gives highly biased results. The adaptive version, however, is able to accurately estimate the log-density for any Mahalanobis distance and is furthermore much faster (it takes only approximately 1 second for a total of $n = 1000$ log-density estimations).

Inspecting the axes in Figures 7 and 8 one can see that our procedure performs well even for very large Mahalanobis distances that would rarely be observed. For likelihood-based methods such as Algorithm 5.4 it is, however, crucial to be able to evaluate the density function for a wide range of inputs. For instance, consider the problem where a sample

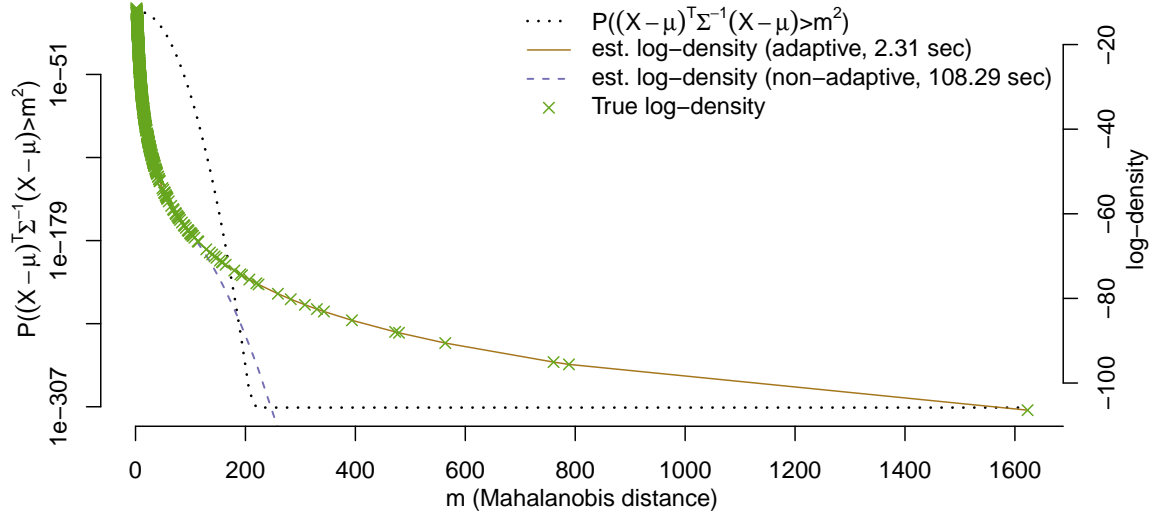


Figure 8 Estimated log-density of $\text{PNMV}_d(\alpha = 2.5, \mathbf{0}, I_d)$ in $d = 10$ evaluated at $n = 1\,000$ points sampled from $\text{PNMV}(\alpha = 0.5, \mathbf{0}, I_d)$.

$\mathbf{X}_1, \dots, \mathbf{X}_n \stackrel{\text{ind.}}{\sim} \text{MVT}_d(\nu, \mathbf{0}, I_d)$ for unknown ν is given. It is then necessary to evaluate the log-density of $\mathbf{X}_1, \dots, \mathbf{X}_n$ at a range of values of ν in order to find the maximum likelihood estimator. In fact, this was the motivation for performing the experiments undertaken to produce Figure 7: The sample is coming from a heavy-tailed multivariate t distribution and the log-density function of a less heavy tailed multivariate t distribution is evaluated at that sample. The same intuition lies behind the experiment to produce Figure 8.

7.4 Fitting normal variance mixture distributions

In this section we provide examples for our fitting procedure Algorithm 5.4. In the case where W follows an inverse-gamma distribution such that $\mathbf{X} \sim \text{MVT}_d(\nu, \boldsymbol{\mu}, \Sigma)$, this problem is not new; see Liu and Rubin (1995) of a discussion of different EM-like algorithms to solve this problem. We compare our Algorithm 5.4 (which approximates all necessary densities and weights) with the an ECME algorithm as provided by the function `fit.mst()` in the R package `QRM` (Pfaff and McNeil (2016)) which uses analytical densities and weights.

Our algorithm is tested in dimensions $d \in \{10, 50\}$ for sample sizes n between 250 and 5 000. In each setting, n random vectors $\mathbf{X}_1, \dots, \mathbf{X}_n \stackrel{\text{ind.}}{\sim} \text{MVT}_d(\nu = 2.5, \mathbf{0}, \Sigma)$ are sampled and then Algorithm 5.4 is used to estimate the parameters. We randomly choose Σ as DRD where R is a random Wishart matrix and D is diagonal with entries $D_{ii} \stackrel{\text{ind.}}{\sim} \text{U}(2, 5)$

7 Numerical Examples

for $i = 1, \dots, d$. Results are displayed in Figure 9 where the estimate $\hat{\nu}$ of ν is plotted as a function of the number of ECME iterations (see Step 2) of Algorithm 5.4). The points at the end of the curves correspond to the (true) maximum likelihood estimators for ν found by the ECME algorithm implemented in the function `fit.mst()`. Note that each single log-density and each single weight in Algorithm 5.4 is approximated via an (adaptive) RQMC algorithm so that long run-times should be expected. It can be confirmed that not only does our procedure converge to the correct maximum likelihood estimator in the given examples, but also that run times are reasonably small for this challenging problem. Note that only few iterations are needed until convergence is detected.

The same test is performed for the Pareto-mixture case, see Figure 10. The symbols at the end of each line display results obtained from Algorithm 5.4 using analytical weights and densities. Again we can confirm that our procedure converges reasonably fast.

The run times displayed in Figures 9 and 10 may seem counterintuitive; however, several factors influence run time: The larger the sample size n , the more integrals need to be approximated and the higher the probability of observing extreme Mahalanobis distances. Furthermore, the problem of estimating the log-density and the weights becomes harder the larger the Mahalanobis distance of the input. However, larger sample sizes can also lead to a quicker convergence of the weights in Step 2.1) of Algorithm 5.4 and also to faster convergence of the estimates of the mixing variable in Step 2.2) of Algorithm 5.4. Overall, as there are numerical approximations involved at many levels, it will depend on the sample at hand how long the algorithm takes. This explains why run times are not monotone in the sample size n .

7.5 Example application

This section demonstrates an application to a real financial data set. We consider stock-return data from constituents of the DowJones30 index; the dataset `DJ_const` is obtained from the R package `qrmdata`, see Hofert and Hornik (2016).

As test distributions to fit to the data we employ a multivariate t distribution and a Pareto-mixture as before and additionally include the multivariate normal distribution. We remark that the latter case is trivial from an estimation point of view (the maximum likelihood estimators for μ and Σ are the sample mean and the sample variance, respectively) but this case is included for the sake of comparison.

We fit the aforementioned distributions to daily, weekly and monthly 30-dimensional log-returns using Algorithm 5.4, once using analytical weights and densities and once using the quantile function as a black box so that all weights and log-densities are estimated. Parameter estimates for the degrees of freedom in the multivariate t case and for the shape parameter α in the Pareto-mixture case along with run times can be found in Table 1.

Observe that the parameter estimates of the underlying mixing distribution are increasing in the length of the time interval over which the returns were calculated. Note that weekly and monthly log-returns are merely sums of daily returns so that some CLT effect takes place. It is known that the distribution function of a multivariate t distribution converges

7 Numerical Examples

Log-returns	Constant		Inverse-gamma		Pareto	
	Analytical	Estimated	Analytical	Estimated	Analytical	Estimated
Daily	- (0 sec)	- (0.39 sec)	3.98 (0.47 sec)	3.96 (19 sec)	1.06 (1.03 sec)	1.06 (10 sec)
Weekly	- (0.17 sec)	- (0.18 sec)	4.53 (0.27 sec)	4.52 (11.47 sec)	1.19 (0.42 sec)	1.19 (2.38 sec)
Monthly	- (0.22 sec)	- (0.13 sec)	8.84 (0.27 sec)	8.8 (2.5 sec)	1.95 (0.42 sec)	1.94 (2.39 sec)

Table 1 Estimates $\hat{\nu}$ for different time frames and different mixing distributions.

to a multivariate normal distribution as $\nu \rightarrow \infty$. If W follows a Pareto distribution with scale 1 and shape ν , it can be seen immediately from the distribution function that $W \rightarrow 1$ in distribution (and thus in probability) as $\alpha \rightarrow \infty$ so that the resulting normal variance mixture converges in distribution to a multivariate normal, too.

Overall it is reassuring that the estimates obtained from analytical and estimated weights and densities only differ slightly; given the difficulty of the problem the run times also seem reasonable.

Figure 11 displays Q-Q Plots of $D^2(\mathbf{x}_i, \hat{\boldsymbol{\mu}}, \hat{\boldsymbol{\Sigma}})$, $i = 1, \dots, n$ as a graphical goodness-of-fit test. Theoretical quantiles are estimated using the methods described in Section 6. The column labels indicate the type of mixing distribution for W . Clearly, the multivariate normal distribution (corresponding to constant W) provides a poor fit to the data as the tail is heavily underestimated. This effect gets less pronounced when moving from daily to monthly return data which is in line with the aforementioned CLT effect. The inverse-gamma mixture provides a reasonably good fit for weekly and monthly return data; the Pareto-mixture has too heavy tails to provide a good fit for daily and weekly data.

Finally, we use Algorithm 3.1 to estimate the joint quantile shortfall probability

$$Q(u) := \mathbb{P}(X_1 \leq F_{X_1}^{\leftarrow}(u), \dots, X_d \leq F_{X_d}^{\leftarrow}(u))$$

for $u \in (0, 1)$. In our context this is the probability that each of the 30 stocks yields a return smaller than its respective u quantile; for small u , $Q(u)$ is the probability of a joint large loss and a rare event. This quantity is often considered in risk management to quantify the risk associated with joint extreme events. Since the margins are continuous, $Q(u)$ is the underlying copula evaluated at (u, \dots, u) . In Figure 12 we plot the estimated quantile shortfall probability $Q(u)$ for a range of values of u for each fitted model separately. The bottom-right figure shows the same probabilities $Q(u)$ standardized by the corresponding normal probability. The plots show again that the Pareto-mixture is more heavy tailed than the multivariate t distribution: It yields significantly higher shortfall probabilities. Furthermore these plots exemplify that our Algorithm 3.1 is also capable of estimating small probabilities despite the increasing numerical difficulty when moving outwards in the joint tail.

7 Numerical Examples

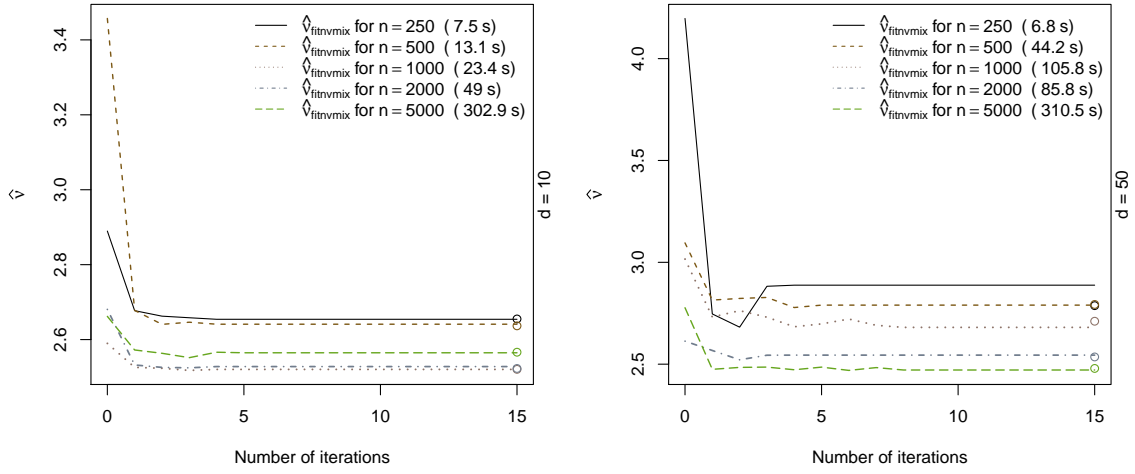


Figure 9 Estimates $\hat{\nu}$ computed by Algorithm 5.4 as a function of the number of ECME iterations for multivariate t distributions of different sample sizes and dimensions. The symbols at the end of each curve denote the maximum likelihood estimator of ν as found by the ECME algorithm with analytical weights and densities.

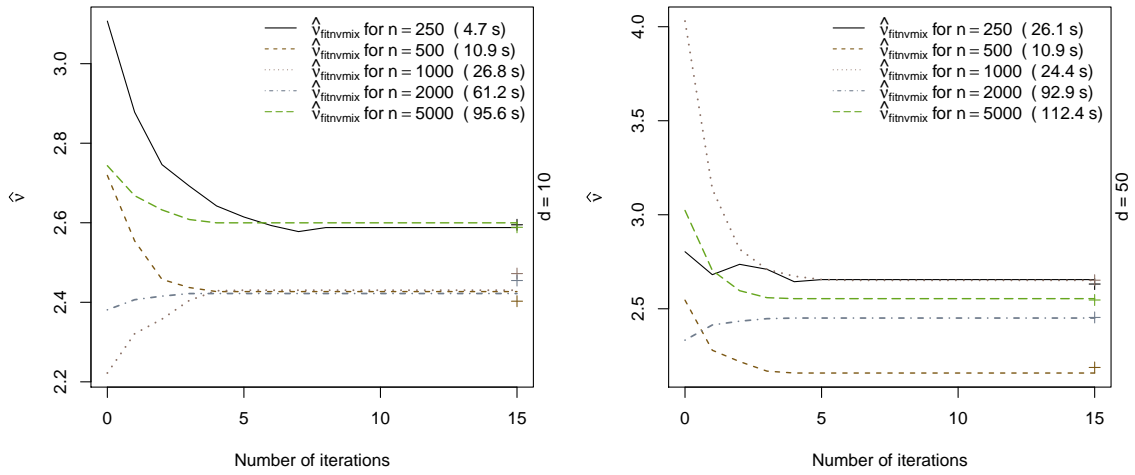


Figure 10 Estimates $\hat{\nu}$ computed by Algorithm 5.4 as a function of the number of ECME iterations for Pareto mixture distributions of different sample sizes and dimensions. The symbols at the end of each curve denote the maximum likelihood estimator of ν as found by the ECME algorithm with analytical weights and densities.

7 Numerical Examples

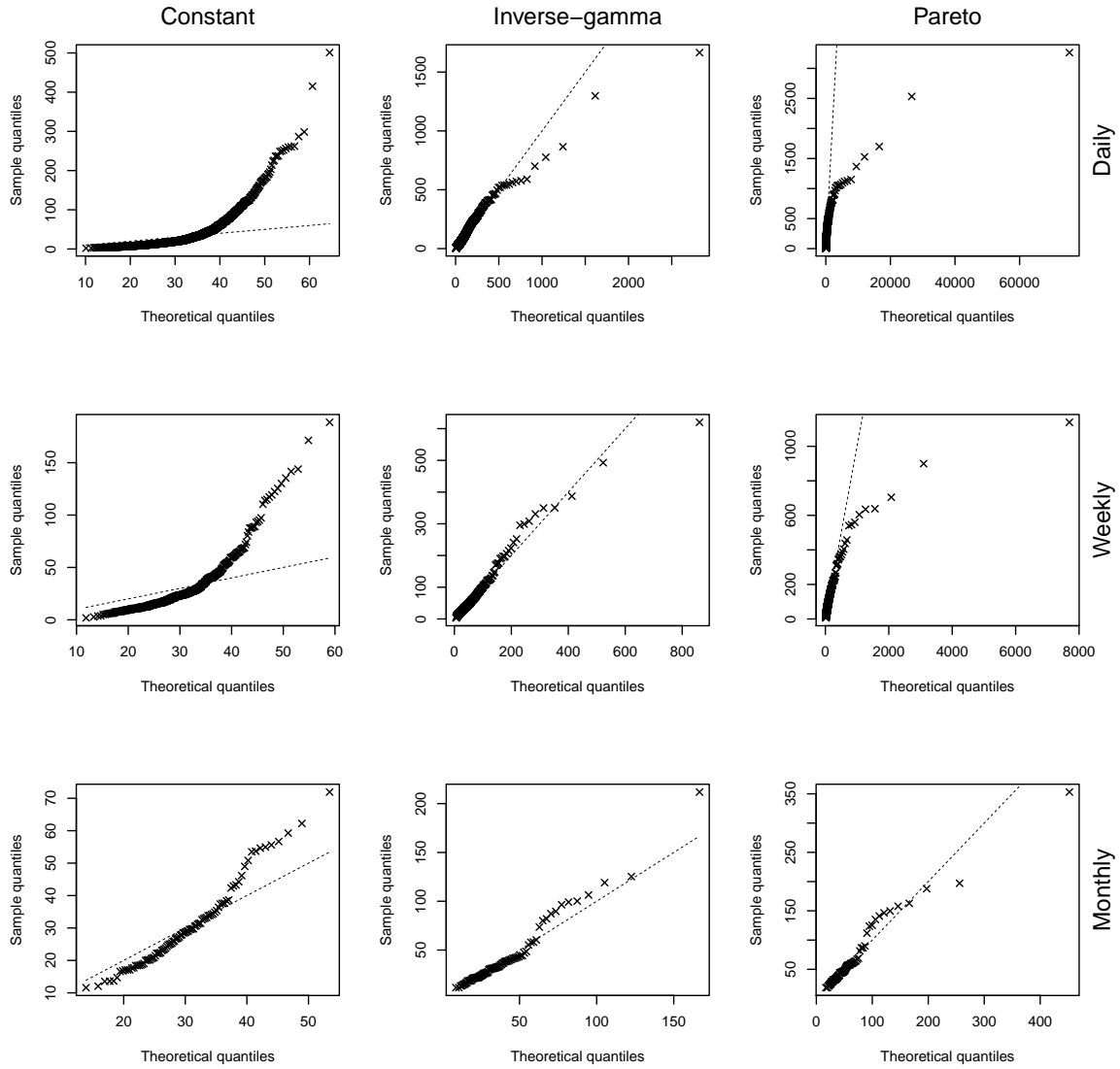


Figure 11 Q-Q Plots of the empirical quantiles of the Mahalanobis distances $D^2(x_i, \hat{\mu}, \hat{\Sigma})$, $i = 1, \dots, n$, versus their theoretical quantiles for different models and time horizons using the DJ_const data set.

7 Numerical Examples

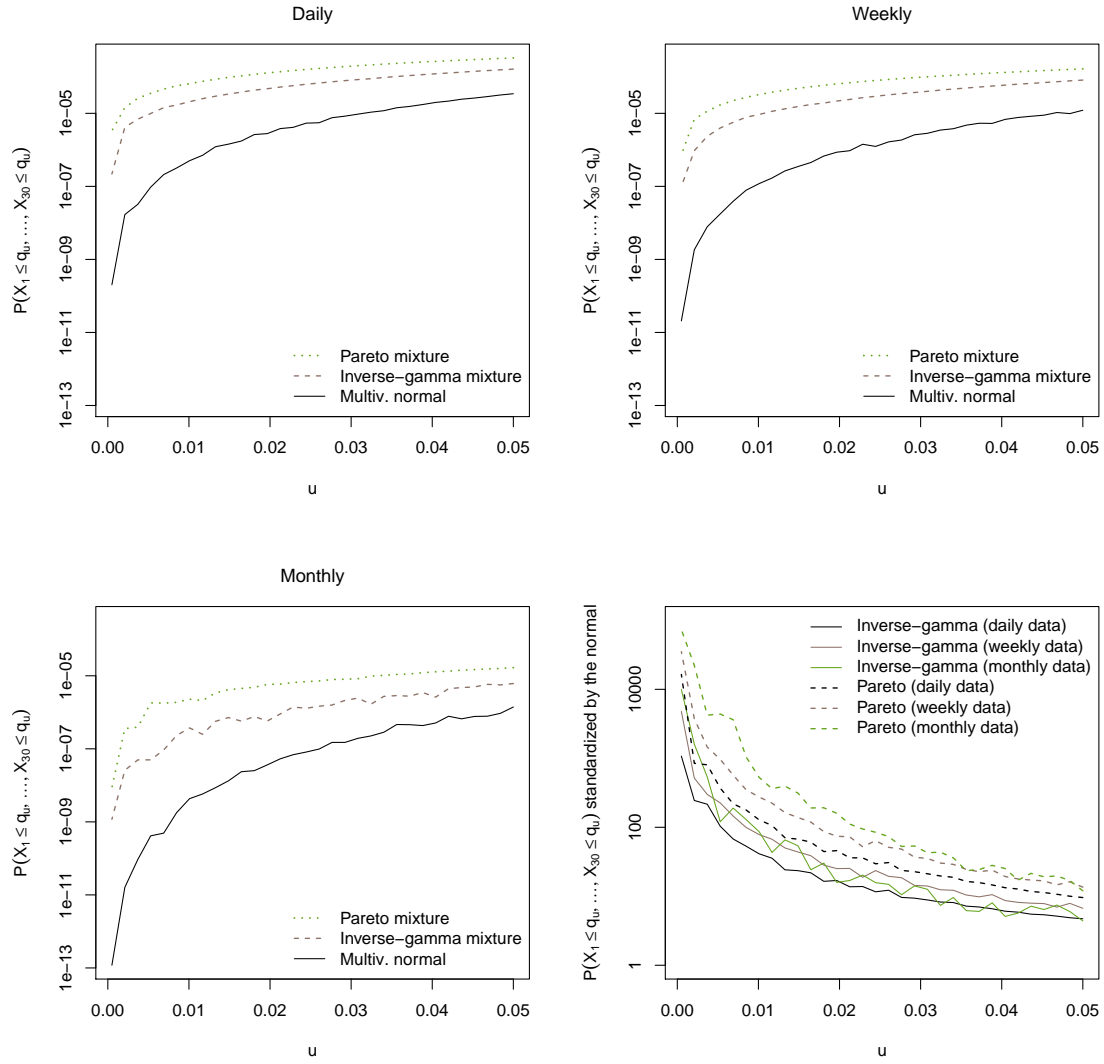


Figure 12 Estimated shortfall probabilities for different models and time horizons using the DJ_const data set.

8 Conclusion

We introduced efficient algorithms to perform the four main tasks for multivariate normal variance mixtures: Estimating the distribution function, the log-density function, sampling and estimating parameters for a given data set when only the quantile function of the mixing variable W is available. Due to the importance of multivariate normal variance mixtures for disciplines such as actuarial science or quantitative risk management, these algorithms are also widely applicable in practice.

We saw that the distribution function and the log-density function of normal variance mixtures can be accurately and quickly estimated even in high dimensions using RQMC algorithms. The algorithm for the distribution function relies on a generalization of methods that were used for estimating multivariate normal and t probabilities in the past, including an efficient variable reordering algorithm. The algorithm for the log-density is based on a RQMC procedure that samples only in important regions. We also saw that it is possible to fit multivariate normal variance mixtures in such generality where all involved quantities such as log-densities and weights need to be estimated using an ECME algorithm. Numerical results validate our methods. An implementation of all methods is provided in the R package `nvmmix`.

We remark that our work also exemplifies the superiority of RQMC methods even in very high dimensions over MC methods for this class of problems.

Another application of our methods is related to normal variance mixture copulas, the implicit copulas derived from normal variance mixture distributions. These copulas can be used to build flexible models with different joint and marginal behaviours. The methods presented here can be used directly to evaluate the distribution and log-density function and for sampling; corresponding methods are implemented in the R package `nvmmix`, too.

A possible limitation of our methods is the assumption of a tractable quantile function of the mixing variable W . For more complicated distributions such quantile function may not be available so that an avenue for future research could be to modify our methods so that they work with a random number generator (RNG) for W (for instance, based on acceptance-rejection algorithms). While sampling and estimating the distribution function is possible when instead of the quantile function of W a RNG for W is provided, this is not the case for estimating the log-density (and thus for the fitting procedure) as our methods are adaptive and thus require sampling in certain low-probability subregions of the support of W .

We also demonstrated via a few examples how variable reordering affects Sobol' indices of the integrand and therefore the effective dimension; given by how much the reordering improves the performance of our RQMC estimator for the distribution function, we believe it would be interesting to explore if this idea can be exploited in other problems as well.

References

- Botev, Z. and L'Écuyer, P. (2015), Efficient probability estimation and simulation of the truncated multivariate student-t distribution, *Proceedings of the 2015 Winter Simulation Conference*, IEEE Press, 380–391, doi:10.1109/WSC.2015.7408180.
- Coffey, C. and Muller, K. (2000), Properties of doubly-truncated gamma variables, *Communications in Statistics-Theory and Methods*, 29(4), 851–857, doi:10.1080/03610920008832519.
- Cranley, R. and Patterson, T. (1976), Randomization of Number Theoretic Methods for Multiple Integration, *SIAM Journal on Numerical Analysis*, 13(6), 904–914, doi:10.1137/0713071.
- Eddelbuettel, D. (2012), Counting CRAN Package Depends, Imports and LinkingTo, <http://dirk.eddelbuettel.com/blog/2012/08/05/> (03/23/2013).
- Genz, A. (1992), Numerical computation of multivariate normal probabilities, *Journal of computational and graphical statistics*, 1(2), 141–149, doi:10.2307/1390838.
- Genz, A. and Bretz, F. (1999), Numerical computation of multivariate t-probabilities with application to power calculation of multiple contrasts, *Journal of Statistical Computation and Simulation*, 63(4), 103–117, doi:10.1080/00949659908811962.
- Genz, A. and Bretz, F. (2002), Comparison of methods for the computation of multivariate t probabilities, *Journal of Computational and Graphical Statistics*, 11(4), 950–971, doi:10.1198/106186002394.
- Genz, A. and Bretz, F. (2009), Computation of multivariate normal and t probabilities, vol. 195, Springer Science & Business Media, doi:10.1007/978-3-642-01689-9.
- Genz, A., Bretz, F., et al. (2019), mvtnorm: Multivariate Normal and t Distributions, R package version 1.0-11, <http://CRAN.R-project.org/package=mvtnorm>.
- Genz, A. and Kwong, K. (2000), Numerical evaluation of singular multivariate normal distributions, *Journal of Statistical Computation and Simulation*, 68(1), 1–21, doi:10.1080/00949650008812053.
- Gibson, G., Glasbey, C., and Elston, D. (1994), Monte Carlo evaluation of multivariate normal integrals and sensitivity to variate ordering, *Advances in Numerical Methods and Applications*, World Scientific Publishing, River Edge, 120–126.
- Glasserman, P. (2013), Monte Carlo methods in financial engineering, vol. 53, Springer Science & Business Media.
- Healy, M. (1968), Algorithm AS 6: Triangular decomposition of a symmetric matrix, *Journal of the Royal Statistical Society. Series C (Applied Statistics)*, 17(2), 195–197, doi:10.2307/2985687.
- Hickernell, F. and Hong, H. (1997), Computing multivariate normal probabilities using rank-1 lattice sequences, *Proceedings of the Workshop on Scientific Computing (Hong Kong)*, 209–215.
- Hofert, M. and Hornik, K. (2016), qrmdata: Data Sets for Quantitative Risk Management Practice, R package version 2016-01-03-1, <https://CRAN.R-project.org/package=qrmdata>.

References

- Hofert, M. and Lemieux, C. (2016), qrng: (Randomized) Quasi-Random Number Generators, R package version 0.0-3, <https://CRAN.R-project.org/package=qrng>.
- Keast, P. (1973), Optimal parameters for multidimensional integration, *SIAM Journal on Numerical Analysis*, 10(5), 831–838, doi:10.1137/0710068.
- Lemieux, C. (2009), Monte Carlo and Quasi - Monte Carlo Sampling, Springer, doi:10.1007/978-0-387-78165-5.
- Liu, C. and Rubin, D. (1994), The ECME algorithm: a simple extension of EM and ECM with faster monotone convergence, *Biometrika*, 81(4), 633–648, doi:<https://doi.org/10.1093/biomet/81.4.633>.
- Liu, C. and Rubin, D. (1995), ML estimation of the t distribution using EM and its extensions, ECM and ECME, *Statistica Sinica*, 19–39, doi:10.1006/jmva.1998.
- McNeil, A., Frey, R., and Embrechts, P. (2015), Quantitative Risk Management: Concepts, Techniques and Tools, Princeton University Press, doi:10.1007/s10687-017-0286-4.
- Mersmann, O. (2015), microbenchmark: Accurate Timing Functions, R package version 1.4-2.1, <http://CRAN.R-project.org/package=microbenchmark>.
- Owen, A. (2013), Better estimation of small Sobol’ sensitivity indices, *ACM Transactions on Modeling and Computer Simulation (TOMACS)*, 23(2), 11, doi:10.1145/2457459.2457460.
- Pfaff, B. and McNeil, A. (2016), QRM: Provides R-Language Code to Examine Quantitative Risk Management Concepts, R package version 0.4-13, <https://CRAN.R-project.org/package=QRM>.
- Pujol, G., Iooss, B., and Janon, A. (2017), sensitivity: Global Sensitivity Analysis of Model Outputs, R package version 1.15.0, <https://CRAN.R-project.org/package=sensitivity>.
- Rosenblatt, M. (1952), Remarks on a Multivariate Transformation, *The Annals of Mathematical Statistics*, 23(3), 470–472, doi:10.1214/aoms/1177729394.
- Sobol’, I. (1967), On the distribution of points in a cube and the approximate evaluation of integrals, *USSR Computational Mathematics and Mathematical Physics*, 7(4), 86–112, doi:10.1016/0041-5553(67)90144-9.
- Sobol’, I. (2001), Global sensitivity indices for nonlinear mathematical models and their Monte Carlo estimates, *Mathematics and computers in simulation*, 55(1-3), 271–280, doi:10.1016/S0378-4754(00)00270-6.
- Wang, X. and Fang, K. (2003), The effective dimension and quasi-Monte Carlo integration, *Journal of Complexity*, 19(2), 101–124, doi:10.1016/S0885-064X(03)00003-7.